Critical opalescence

L. A. Zubkov and V. P. Romanov

A. A. Zhdanov Leningrad State University

Usp. Fiz. Nauk **14**, 615–659 (April 1988)

Studies of critical opalescence near phase transitions in different systems are reviewed. The fundamentals of the modern approach to the description of the propagation and scattering of light in media with large nonuniformities are presented. The experimental data on the coefficient of extinction and integrated intensity of the scattered light are analyzed and different models for the correlation function are discussed. Different methods for studying multiple scattering of light and methods for eliminating it from the measured intensity are examined. The kinetic properties of systems in the critical region are examined. Attention is devoted primarily to the experimental data obtained by the methods of correlation spectroscopy and to the comparison of these data with the predictions of different theoretical models. Significant attention is devoted to the study of phase transitions in liquids by the methods of light scattering as well as the problem of propagation and scattering of light in the nematic phase, where fluctuations of the director exhibit the same behavior as at the critical point. In conclusion, phase transformations in micellar solutions, to which a great deal of attention has been devoted in recent years, are studied.

CONTENTS

INTRODUCTION

As the points of liquid-liquid and liquid-vapor equilibrium are approached optically transparent systems start to become cloudy owing to strong scattering of light. This phenomenon is well known and is termed critical opalescence. The optical properties of such systems depend strongly on the closeness to the critical point, and for this reason the method of light scattering is widely employed in the study of second-order phase transitions and critical phenomena.[1a)] This method has the significant advantage that in studying the intensity of the scattered light there is virtually no external perturbation acting on the system, and fluctuations of the order parameter make the main contribution to the scattering, since they grow in an unbounded fashion as the transition point is approached. For this reason, the values of the critical parameters, obtained from such experiments are in this sense most reliable.

One of the main problems in the theory of phase transitions is the calculation of the critical indices of different physical quantities and the amplitudes corresponding to them. This is done with the help of different modifications of the renormalization group method or high-temperature expansions. The criterion for the validity of some particular approach is the direct comparison of the computational results with the experimental data. Since the difference in the values of the parameters obtained theoretically is, as a rule, not large, the experiments must meet very exacting requirements.

Critical opalescence experiments are of two types. In one type the equilibrium properties of systems are studied, while in other types the time correlation function of the fluctuations of the order parameter is studied. In both cases, in addition to the problem of maintaining a constant temperature, which is common to all experiments on critical phenomena, there appear specific requirements on light sources and systems for recording the scattered radiation.

Aside from purely technical problems, there also appear problems of a fundamental character. Information about the critical parameters appears in the simplest possible manner in the single scattering of light. Very close to the critical point, within hundredths or thousandths of a degree, however, higher-order scattering begins to play an appreciable role in most objects. The contribution of multiple scattering can be reduced appreciably in a purely experimental

 0038-5670/88/040328-26$01.80

fashion, but it cannot in principle be eliminated completely from the total intensity. Methods enabling separation of purely single-scattering have therefore been developed. It has turned out that for this additional measurements must be performed and the problem of light scattering in the real geometry of the experiment must be solved.

Critical opalescence has now been studied in greatest detail near the critical point of separation and the liquid-vapor point, which are equivalent second-order phase transitions. These transitions have been most fully described theoretically, and the main efforts are directed toward clarifying the fine details of the phase transition. The optical diversity of these systems has made it possible to develop the entire experimental procedure to a very high standard.

As a result, it is now possible to study even more complicated systems. This concerns, first of all, liquid crystals, in which a great deal of attention is devoted to the study of the isotropic liquid—nematic liquid crystal transition. This phase transition is unusual in that because of the low heat of the transition the pretransition phenomena are observed over a wide temperature interval and, in the process, the behavior of the susceptibility does not exhibit any universality.

The nematic phase is also interesting from the viewpoint of critical opalescence. The spectrum of the fluctuations of the director is a Goldstone spectrum with an anomalously large long-wavelength part, so that the scattering of light over the entire region of existence of this phase occurs in the same manner as at the critical point itself, which is not attainable in order physical systems.

The intensive study of the critical behavior of a wide class of micellar systems has been initiated in the last few years because of the great practical applications of these systems. Extensive experimental data, for which it is not always possible to find a rational explanation, have been accumulated in this field.

In this review we shall try to study all these objects from a unified viewpoint and identify the general results that unify them. A relatively large amount of attention is devoted to the problems of designing experiments and the concomitant methodological questions, since it is precisely the solution of these problems that in many cases makes it possible to obtain reliable results. The theory of light propagation, including also multiple propagation, is presented only to the extent that is necessary for the analysis of experimental data and the discussion of the results obtained, since these questions have been studied in detail in many reviews and monographs (see, for example, Refs. 1b and 2). We shall also virtually ignore the characteristics of light scattering near the liquid-vapor critical point, where the gravitational effect plays a significant role, since this problem has been discussed in detail in a recent review.[3]

1. PROPAGATION AND SCATTERING OF LIGHT IN A NONUNIFORM MEDIUM

The phenomenological theory of light scattering is based on Maxwell's equations. We shall neglect the magnetic properties of the medium. The relationship between the electric induction vector $\mathbf{D}$ and the electric field intensity vector $\mathbf{E}$ is assumed to be linear and local

$$\mathbf{D}(\mathbf{r}, t) = \varepsilon(\mathbf{r}, t)\,\mathbf{E}(\mathbf{r}, t), \tag{1.1}$$

where the dielectric permittivity, for simplicity assumed to be scalar,

$$\varepsilon(\mathbf{r}, t) = \varepsilon_0 + \delta\varepsilon(\mathbf{r}, t), \tag{1.2}$$

consists of a constant part ε_0 and a fluctuating part $\delta\varepsilon(\mathbf{r}, t)$. The quantity $\langle \delta\varepsilon(\mathbf{r}, t)\rangle = 0$, where the brackets $\langle \ldots \rangle$ denote statistical averaging.

In the case when the incident wave is the source of the field, it is possible to transfer from Maxwell's equations to the equivalent integral equation

$$E_\alpha(\mathbf{r}, t) = E_{0\alpha}(\mathbf{r}, t) + \int d\mathbf{r}_1\, dt_1\, T^0_{\alpha\beta}(\mathbf{r}-\mathbf{r}_1, t-t_1) \times \delta\varepsilon(\mathbf{r}_1, t_1)\, E_\beta(\mathbf{r}_1, t_1), \tag{1.3}$$

where $T^0_{\alpha\beta}$ is the dipole propagator, whose Fourier transform equals

$$T^0_{\alpha\beta}(\mathbf{r}, \omega) = \frac{1}{4\pi\varepsilon_0}\left[\left(\frac{\omega n_0}{c}\right)^2 \delta_{\alpha\beta} + \frac{\partial^2}{\partial r_\alpha\, \partial r_\beta}\right]\frac{1}{r}\exp\left(i\frac{\omega}{c}n_0 r\right); \tag{1.4}$$

ω is the circular frequency, c is the velocity of light in a vacuum, $n_0^2 = \varepsilon_0$, and $\mathbf{E}_0(\mathbf{r}, t)$ is the electric field intensity vector, satisfying Maxwell's equations with $\delta\varepsilon(\mathbf{r}, t) = 0$ and the corresponding boundary conditions.

The iterative solution of Eq. (1.4) can be represented in the diagramatic form:

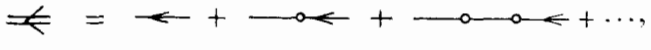

(1.5)

where the diagramatic representations of $\mathbf{E}$, $\mathbf{E}_0$, $\hat{T}^0$, $\delta\varepsilon$ are as follows:

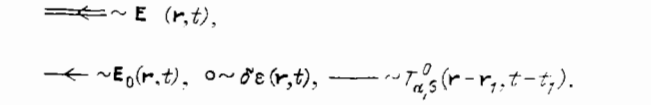

At every vertex O integration over space and time and summation over all polarizations are performed; the left end of every diagram corresponds to the point $(\mathbf{r}, t)$.

We shall be interested in the average field in the medium and the scattering intensity:

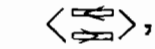

defined by the mutual coherence tensor $\langle E\alpha(\mathbf{r}, t)\, E^*_\beta(\mathbf{r}, t)\rangle$. Averaging (1.5), we obtain

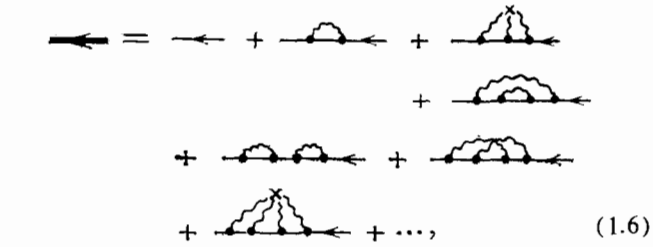

(1.6)

where

denote the irreducible correlation functions $\langle \delta\varepsilon(\mathbf{r}_1, t_1)\, \delta\varepsilon(\mathbf{r}_2, t_2)\rangle$, $\langle \delta\varepsilon(\mathbf{r}_1, t_1)\, \delta\varepsilon(\mathbf{r}_2, t_2)\, \delta\varepsilon(\mathbf{r}_3, t_3)\rangle$. For a fluctuating medium the dipole propagator

is introduced analogously.

We note that in the far zone $\mathbf{r} \gg \lambda$, where λ is the wavelength of the light wave, the form of the dipole propagator is the same as that of $T^0_{\alpha\beta}$ with ε_0 replaced by ε—the dielectric permittivity of the medium. The wavelength-dependent difference $\varepsilon - \varepsilon_0$ can be expressed as the spatial Fourier transform of the collection of diagrams[1b)]

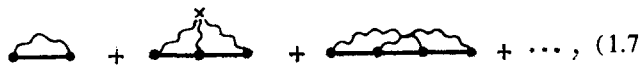

(1.7)

regarded as a function of the difference of the coordinates of their ends. Averaging the squared combination of the fields (1.5) we obtain the intensity of the scattered light:

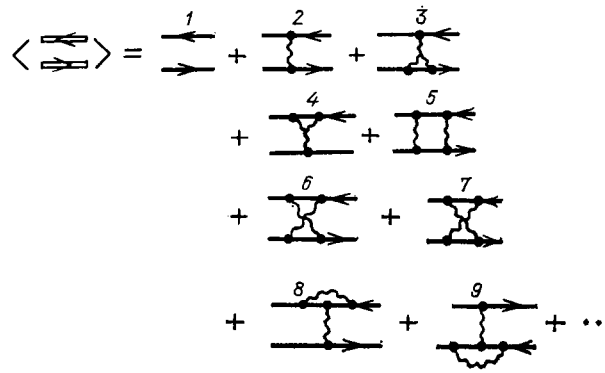

(1.8)

Here partial summation of the diagrams has been performed, so that the answer is expressed in terms of the average field and the average propagator. The second diagram describes the single-scattering of light. The third and fourth diagrams are termed sesquiscattering, and the fifth diagram describes double-scattering. The remaining diagrams can also be referred to double-scattering, but, unlike the fifth diagram, because of correlations they are linked with processes localized in a bounded region of space, like the third and fourth diagrams.

In what follows we shall study only the second and fifth diagrams and the analogous ladder diagrams of higher order, since the main contribution to scattering is linked precisely with three diagrams.[4]

Let us examine the parameter with respect to which the expansion in the orders of scattering is performed. The fifth diagram, compared with the second diagram, contains the factor

$$\Delta \sim \int d\,\mathbf{r}_1\, d\mathbf{r}_2 T\,(\mathbf{r}_3 - \mathbf{r}_1)\; T\,(\mathbf{r}_4 - \mathbf{r}_2)\; \langle \delta a_i\,(\mathbf{r}_1)\, \delta a_i\,(\mathbf{r}_2)\rangle. \tag{1.9}$$

Here it is assumed that the fluctuation of the dielectric permittivity depends linearly on the fluctuations of the thermodynamic quantities a_i.

$$\delta\varepsilon\,(\mathbf{r},\, t) = \frac{\partial\varepsilon}{\partial a_i}\,\delta a_i\,(\mathbf{r}_i\, t). \tag{1.10}$$

Outside the critical region

$$\Delta \sim \frac{L l_0^3}{\lambda^4}, \tag{1.11}$$

where L is the characteristic size of the scattering system and l_0 is a distance of the order of the intermolecular separation. In obtaining this estimate we took into account the fact that $|\mathbf{r}_3 - \mathbf{r}_4| \sim l_0$.

On transferring into the critical region the fluctuations of the order parameter $\delta c(\mathbf{r})$, whose correlation function $\langle \delta c(\mathbf{r}_1)\, \delta c(\mathbf{r}_2)\rangle$ becomes long-ranged, make the main contribution to the scattering. In this case the characteristic scale l_0 is replaced by the correlation radius $r_C = r_0\, \tau^{-\nu}$, which increases as the critical point is approached; here $\tau = |T - T_c|/T_c$, where T_c is the critical temperature, ν is the critical index, and r_0 is a quantity of the order of several angstroms. Since the correlation function itself decays even at the critical point itself approximately as $1/r$, the substitution $l_0^3 \to r_C r^2$, occurs in the expansion parameter, i.e.,[5]

$$\Delta \sim \frac{L r_0 r_C^2}{\lambda^4}. \tag{1.12}$$

This estimate shows that the contribution of higher-order scattering increases as the critical point is approached and, as in (1.11), depends on the dimensions of the scattering system.

Under the conditions of critical opalescence the integrated intensities of single- and double-scattering of light by fluctuations of the order parameter in the case of an incident monochromatic plane wave have, according to (1.8), the form

$$I^{\alpha(1)}_{\beta(C)} = \frac{I_0}{X^2}\, R_{sc(C)} V \left(\delta_{\alpha\beta} - \frac{k_{p\alpha} k_{p\beta}}{k^2}\right)^2 G_{(C)}(q), \tag{1.13}$$

$$I^{\alpha(2)}_{\beta(C,C)} = \frac{I_0}{X^2}\, R^2_{sc(C)} \int_{V_1} d\mathbf{r}_1 \int_{V_2} d\mathbf{r}_2\, \frac{1}{|\mathbf{r}_1 - \mathbf{r}_2|^2} \times [\delta_{\alpha\beta} - m_\alpha m_\beta - n_\alpha n_\beta + (mn)\, m_\alpha n_\beta]^2\, G_C(\mathbf{q}_1)\, G_C(\mathbf{q}_2). \tag{1.14}$$

Analogous expressions can be written down for the higher-order scattering. In (1.13) and (1.14) $R_{sc(C)}$ is the scattering constant, $G_C(q) = \langle |C_q|^2\rangle \times \langle |\delta C_{q=0}|^2\rangle^{-1}$ is the q-dependent part of the correlation function of the fluctuations of the order parameter.[1)] α and β are the polarizations of the incident and scattered light, k is the wave number, V is the observed part of the illuminated volume, V_1 is the entire illuminated volume, V_2 is the volume from which the scattered light strikes the recording apparatus, X is the distance up to the point of observation, $\mathbf{q} = \mathbf{k}_i - \mathbf{k}_s$ is the wave vector of the scattering fluctuation mode, $q = 2k \sin(\theta/2)$, θ is the scattering angle, $\mathbf{k}_i$ and $\mathbf{k}_s$ are the wave vectors of the incident and scattered light in $I^{(1)}$, $n = \mathbf{X}/X$ is the direction to the point of observation, $\mathbf{q}_1$ and $\mathbf{q}_2$ are the scattering wave vectors in $I^{(2)}$, $k\mathbf{m}$ is the wave vector of the light wave during intermediate reradiation, and $\mathbf{m} = (\mathbf{r}_2 - \mathbf{r}_1)/|\mathbf{r}_2 - \mathbf{r}_1|$. The formulas (1.13) and (1.14) were derived under the assumption that the distance up to the point of observation is much larger than the dimensions of the scattering system, while the characteristic frequency of the fluctuations of the order parameter is much smaller than the frequency of the incident light. The standard arrangement of the light-scattering experiment is shown in Fig. 1. The incident beam and the recorded scattered light lie in a horizontal plane. The incident beam is either vertically (E^V) or horizontally (E^H) polarized, and scattered light whose polarization vector is orthogonal to the scattering plane (E_V) or lies in it (E_H) is recorded.

Scattering attenuates light beams:

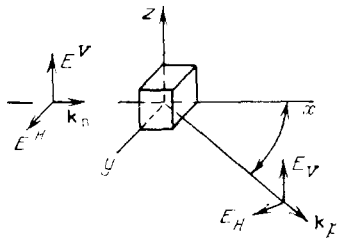

FIG. 1. Arrangement of the light-scattering experiment.

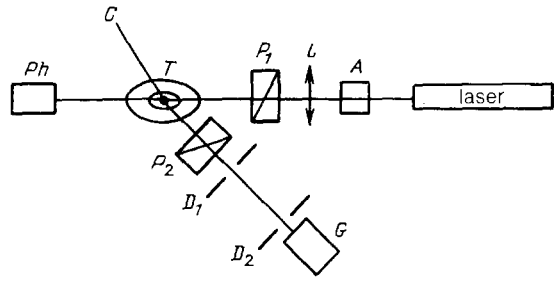

FIG. 2. Overall view of the apparatus for studying critical opalescence. A) device enabling stabilization of the incident radiation; Ph) photodetector measuring the intensity of the transmitted light; G) apparatus recording the scattered radiation, including a photodetector with a system for storing and processing data, a correlator, spectrum analyzer, and Fabry-Perot interferometer; P_1, P_2) polarizers; D_1, D_2) diaphragms; L) lens; T) temperature stabilizing apparatus on a goniometer; C) cell holding the liquid under study.

$$I = I_0 e^{-\sigma l},$$

where l is the path traversed by the light in the medium and σ is the extinction coefficient. Extinction not only attenuates the light passing through the system, but it must also be taken into account in the solution of the problem of light scattering. To calculate the extinction coefficient in the lowest order approximation one can either integrate the intensity of the scattered light from a unit length of the beam over the entire solid angle[6] or calculate the imaginary part of the fluctuation contribution to the dielectric permittivity the first diagram in (1.7).[1b]

The information about the critical behavior of the system that is obtainable from light-scattering experiments can be easily demonstrated with the help of the Ornstein-Zernike approximation for the correlation function:

$$\langle |C_{\mathbf{q}}|^2 \rangle = \frac{\langle |\delta C_{\mathbf{q}=0}|^2 \rangle}{1 + (qr_C)^2}, \qquad (1.15)$$

where $\langle |\delta C_{\mathbf{q}=0}|^2 \rangle \sim \tau^{-\gamma}$; here γ is the critical index of the susceptibility.

The formulas (1.13) and (1.15), taking into account the fact that $R_{sc} \sim \langle |\delta C_{\mathbf{q}=0}|^2 \rangle$, imply that far from the critical point the intensity of the scattered light grows as $\tau^{-\gamma}$. As the transition point is approached this growth slows down owing to the increases in qr_C, the light scattering starts to depend on the angle, and the region of small angles starts to make the main contribution. Therefore light scattering experiments make it possible, in principle, to find the index of the susceptibility and measure the correlation radius, i.e., find the indices γ and ν and the quantity r_0, as well as to determine the small index η, related with γ and ν by the relation $2 - \eta = \gamma/\nu$. In addition, the kinetic phenomena discussed in Sec. 5 can be studied.

2. METHODS FOR STUDYING CRITICAL OPALESCENCE

The general experimental arrangement for studying critical opalescence or the spectral composition of the scattered light is shown in Fig. 2. The light source is usually a continuous gas laser, which together with stabilizing devices of different types enables maintaining the radiation power constant to within several tenths of a percent. The stabilizing devices are of two types. In one type a photodetector is inserted into the feedback system, which enables maintaining the radiation power constant with a fixed accuracy.[7,8] With the other devices the intensities of the transmitted and scattered light are measured in units of the incident light.

The radiation power is selected so that the heating of the sample owing to absorption of light would not exceed the temperature stabilization error. The heating for the standard weakly absorbing liquids far from the edge of the absorption band does not exceed $(2–5) \cdot 10^{-4}$ deg/mW.[7,9] For this reason an He-Ne laser with a wavelength of $\lambda = 6328$ Å is most often employed.

The sizes of the cells holding the substance under study vary from fractions of a millimeter[10] up to several centimeters,[7,8,11] depending on its scattering properties. The use of large cells makes it much easier to align the optical part of the apparatus, which is especially important for performing angular measurements. In addition, in this case the contribution of different types of reflections and bright spots at the interfaces of different media is appreciably smaller. Cells always contain, together with the incident beam, a beam reflected from the output window of a cell of any size, the scattered light from which must either be taken into account in the analysis of the experimental data[7] or must be substantially attenuated, for example, by gluing a neutral filter to the outer side of the cell.[8]

The systems studied are prepared from chemically pure preparations and foreign inclusions are without fail removed from them either by vacuum distillation or filtering through filters with pore sizes of 0.2–0.5 μm.

For each concrete system studied preliminary experiments must be performed in order to determine the position of the critical point. In the case of solutions the critical concentration C_c is determined from an analysis of the data on the coexistence curve, while the critical temperature T_C is determined from the moment at which an interface appears between phases as the temperature is varied from the side of the single-phase region. For solutions in which the difference between the refractive indices of the components is very small the position of T_C is determined from the change in the intensity of the scattered light as a function of the temperature. The temperature is varied discretely, and the accuracy of determination depends on the step size.[9]

In the last few years, with the appearance of high-quality electronics, great progress has been achieved in stabilizing and measuring the temperature. The cell is placed into a double or triple thermostat, the temperature of whose outer jackets is somewhat lower than the interior temperature. The temperature is maintained constant with the help of a bridge circuit, whose active element is a temperature-sensitive resistance. The internal thermostat is often made of copper, which enables appreciable reduction of the temperature

gradients in the cell. The temperature of the system under study is measured with the help of platinum or quartz thermometers. In modern thermostats the precision with which the temperature is maintained reaches $2 \cdot 10^{-4}$ deg.

When measurements are performed in a wide range of angles the light source and the thermostat with the cylindrical cell are usually immobile, while the collimating and receiving apparatus is moved with the help of a goniometer. The collimating apparatus, consisting of a set of diaphragms that limit the scattered-light aperture, is aligned so as to receive light from the center of the cell.

In studies of the integrated intensity the scattered light strikes a photodetector, which serves as an input element for the recording apparatus. The main requirement imposed on this apparatus is that it must be linear over the entire range of measured light intensities and it must operate in a stable fashion during the experiment. Recording devices now usually operate in the photon counting mode, so that this method makes it possible to achieve the required signal-to-noise ratio by accumulating the useful signal.

Two types of apparatus are employed in the analysis of the spectral composition of the scattered light: optical heterodyning, described in detail in Ref. 12, is employed at frequencies below 10^6 Hz, while for frequencies of 10^6–10^{12} Hz a Fabry-Perot interferometer is employed as the spectral apparatus. Multipass Fabry-Perot interferometers, whose degree of contrast, for example, reaches 10^8–10^9 for a triple-pass etalon,[13] are often employed.

3. DETERMINATION OF THE CORRELATION FUNCTION FROM THE LIGHT-SCATTERING DATA

The equilibrium properties of systems near the critical point can be studied by analyzing the temperature dependence of the extinction coefficient or by measuring the integrated intensity of the scattered light at one or several angles. Each of these experiments has specific features that we shall discuss in this section.

3.1. Study of extinction coefficients

Experimental investigations in which the intensity of the transmitted light is studied have many common features. In practice the measurements are always performed by the compensation method[6,9,14–16] based on the optical analog of the Wheatstone bridge, i.e., the intensities of the incident and transmitted light are compared. The accuracy of the measurements is quite high, better than 1%. The simplicity of the optical part of the apparatus, including also the cell holding the liquid under study, enables increasing appreciably the accuracy of temperature stabilization and thereby approach closer to T_c. For example, $\tau \sim 10^{-7}$ was achieved in Ref. 9.

From these experiments the temperature dependence of the extinction coefficient is determined. The typical results

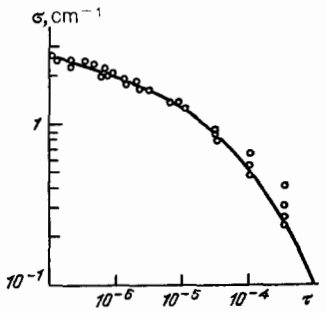

FIG. 3. Temperature dependence of the extinction coefficient of a binary mixture of methanol and cyclohexane.[9]

of such measurements are presented in Fig. 3. The extinction coefficient has the following scaling:

$$\sigma = \sigma_0 \tau^{-\gamma} f(kr_C). \tag{3.1}$$

The experimental data are usually analyzed by using the explicit expression for σ, derived with the help of the Ornstein-Zernike approximation:

$$\sigma = \frac{\pi}{2} B \left[\left(2 + x^{-2} + \frac{1}{4} x^{-4}\right) \ln (1 + 4x^2) - 2 - x^{-2} \right]$$

$$\equiv \frac{\pi}{2} B \psi(x), \tag{3.2}$$

where $B = R_{sc}/x^2$ and $x = kr_C$. In this case

$$\sigma_0 = \pi B k^2 r_0^2,$$
$$f(kr_C) = \frac{1}{2} (kr_C)^{-2} \psi(kr_C). \tag{3.3}$$

It is obvious from the expression for σ that the parameters γ, ν, r_0, and σ_0 (or B) can in principle be determined from the optical data. As one can see from Fig. 3, however, the dependence $\sigma(\tau)$ is a smooth curve, and it is therefore possible to determine only some of these parameters, while the others are taken from other independent experiments or from the theory. It is precisely for this reason that the simplest Ornstein-Zernike approximation is employed to describe the extinction experiments.

The temperature dependence of σ was first used in Ref. 6 to determine the values of the critical parameters. In this work all four parameters of sulfur hexafluoride were determined near the liquid-vapor critical point. The results showed that since the illuminated volume is much smaller than the cell, gravity has a much smaller effect than in PVT measurements. In Ref. 6 the gravitational effect started to appear only for $T - T_c < 0.04$ K.

The extinction of a strongly opalescing mixture of methanol and cyclohexane was studied by Kopelman and Gammon.[9] Only two parameters r_0 and σ_0 were determined, while γ and ν were assumed to be constant. Kopelman and Gammon pointed out that among different types of experiments, such as measurement of the heat capacity and light

TABLE I. Critical parameters for sulfur hexafluoride found from measurements of the extinction coefficient.[6]

ν	γ	r_0	η
0.67±0.07	1.225±0.002	1.5±0.23 Å	0.15±0.22

scattering, the spread in the values of r_0 is significant, though the values of the critical parameters are close. The extinction data agree best with the measurements of the heat capacity.[17] The more complicated form of the correlation function, obtained from the results of Ref. 7, was employed in Ref. 14 to study the extinction in the binary systems isobutyl alcohol—water and aniline—cyclohexane. The values of γ and ν were also fixed. The results of these experiments showed that the small index η cannot be determined from the temperature dependence of the extinction coefficient.

3.2. Single-scattering

As we can see, the entire set of critical parameters cannot be determined with high accuracy from the extinction data. For this reason, in performing experiments to determine the form of the correlation function the intensity of the scattered light is studied. If the critical isochore is studied for a liquid-vapor system or a binary mixture with a critical concentration, then the correlation function quite close to the critical temperature can be written in the scaling form as[18]

$$\chi(\tau,k) = A\tau^{-\gamma}G(kr_c), \tag{3.4}$$

where A is a numerical coefficient. The universal function $G(x)$ satisfies the limiting conditions[19-21]

$$\begin{aligned} G(x) &= \frac{1}{1+x^2} \quad \text{for} \quad x \ll 1, \\ G(x) &= \frac{C_1}{x^{2-\eta}}\left(1+\frac{C_2}{x^{(1-\alpha)/\nu}}+\frac{C_3}{x^{1/\nu}}\right) \quad \text{for} \quad x \gg 1. \end{aligned} \tag{3.5}$$

The values of the coefficients C_1, C_2, and C_3 can be calculated by the ε-expansion method.[22]

To analyze the experimental data the form of the correlation function must be known for all values of x, and not only in the limiting cases. In the early experimental works, devoted to the study of the form of the correlation function and finding the small index η, the data on the light-scattering intensity were interpreted on the basis of Fisher's approximation

$$G(x) = (1+x^2)^{-[1-(\eta/2)]}. \tag{3.6}$$

Although this formula satisfies the limiting conditions (3.5), i.e.,

$$G(x) \sim \text{const} \quad \text{as} \quad x \to 0, \quad G(x) \sim x^{\eta-2} \quad \text{as} \quad x \to \infty,$$

for finite values of x it can give only an approximate description of an experiment. For this reason finding the small index η from the formula (3.6) can lead to appreciable errors.

The form of the correlation function was studied experimentally in greatest detail by Chang *et al.*[7] The results on the intensity of light scattering were obtained for a weakly opalescing segregating solution of 3-methyl pentane—nitroethane with the refractive indices of the components of the mixture differing by $\Delta n = 0.0129$ in the temperature range $10^{-6} < \tau < 2.7 \cdot 10^{-3}$, $T_c = 299.545 \pm 0.002$ K, and $C_c = 0.5$ mole %. The heating by an He-Ne laser did not exceed 0.22 mK/mW. A double thermostat ensured that the temperature in the cylindrical cell 1 cm in diameter and 6 cm high was maintained constant with an accuracy of the order of 0.3 mK. The temperature gradient equalled about 0.2 mK/cm. The measurements were performed at one scattering angle $\theta = 90°$. The observed illuminated volume equalled $V = 0.95$ mm^3.

The intensity of the scattered light was represented in this experiment in the form

$$I = I_0(1+6{,}4\tau)[1-(1-R^{(2)})\sigma l]\tau^{-(2-\eta)\nu}G(kr_c)+\Delta I. \tag{3.7}$$

In this expression the first term describes the light scattering by fluctuations of the order parameter, for which the mole fraction of one of the components of the mixture or its volume concentration can be employed. The factor in brackets takes into account the correction for extinction (σl) and multiple scattering (R^2). The quantity $R^{(2)}$, as a function of kr_c, was calculated in the double scattering approximation.[23] This question will be discussed in greater detail below. The relative contribution of σ and $R^{(2)}$ varied from 0.4% at $\Delta T = 0.1$ K up to 3.8% for $\Delta T = 0.3$ mK. The factor $1 + 6.4\tau$ is responsible for the temperature dependence of the refractive index. It was calculated using the Clausius-Mossoti formula and taking into account the corrections for volume mixing. The term ΔI accounts for the noncritical contribution to the scattering by pressure and temperature fluctuations. In this work ΔI was assumed to be constant and for $\Delta T = 1$ K equalled 10% of the total intensity of light scattering.

The experimental data were analyzed with the help of several types of correlation functions. In particular,

$$G^{-1}(x) = 1 + x^2\left(1+\frac{1}{\eta}x^2\right)^{-\eta/2}(1+\eta S(x)), \tag{3.8}$$

where the function S depends not only on kr_c, but also on ν, η, C_2, and C_3. In addition, the correlation function obtained from the analysis of experimental data on the three-dimensional Ising model was used:

TABLE II. Critical parameters found with the use of different forms of the correlation functions.[7]

Method of determination	Critical parameters				Accuracy of description, %
	η	ν	γ	r_0, Å	
From experiment by substitution of (3.8) into (3.7)	0.017±0.015	0.625±0.006	1.240±0.017	2.29±0.10	0.4
Substitution of (3.9) into (3.7)	0.024±0.022	0.625±0.006	1.235±0.016	2.28±0.12	0.4
Substitution of $G(x)$ from Ref. 24 into (3.7)	0.029±0.017	0.625±0.006	1.238±0.018	2.28±0.10	0.4
Approximate (Orstein-Zernike)	0	0.633±0.008	1.266±0.017	2.22±0.13	0.5

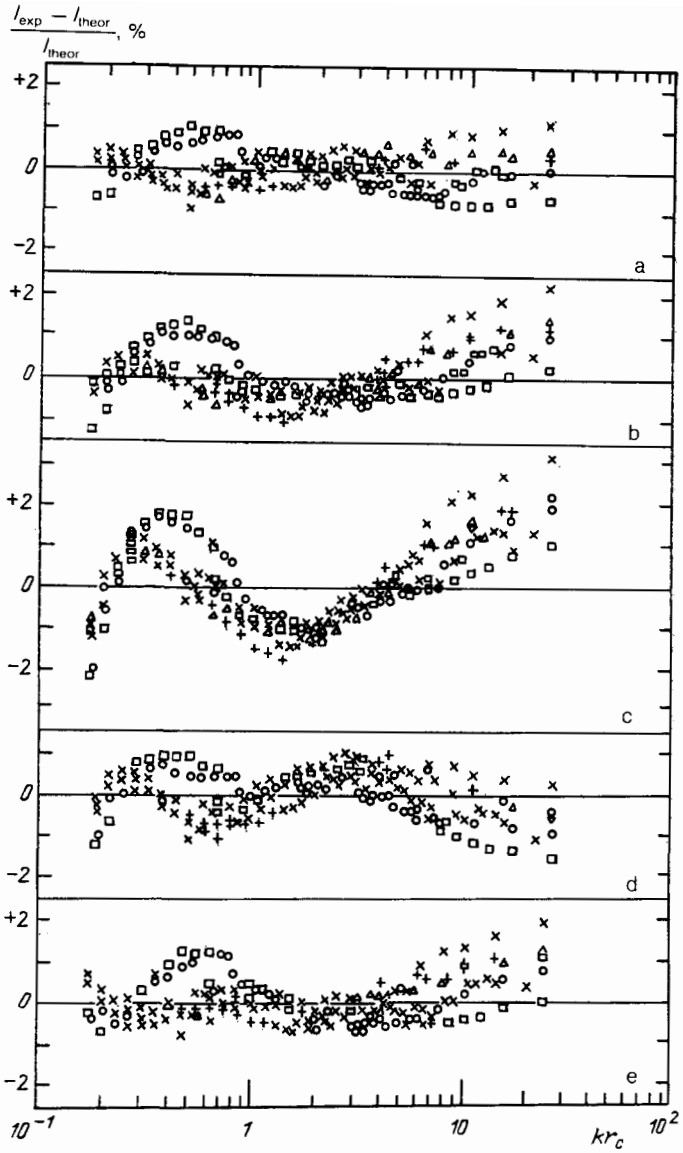

FIG. 4. The degree of deviation of the experimental data on the light-scattering intensity[7] from the theoretical values calculated by different methods as a function of kr_c. a–c) substitution of (3.8) into (3.7) with the parameters in the first row of Table II (a), determined by renormalization group methods[25,26] (b), from temperature expansions[27] (c). d) substitution into (3.7) of the Ornstein-Zernike formula with $\eta = 0$, $\nu = 0.633$, $\gamma = 2\nu$, $r_0 = 2.22$ Å. e) substitution of the renormalization group parameters with the asymptotic corrections in the form (3.10) and (3.11).

$$G(x) = \frac{[1+(\psi^2/x^2)]^{\eta/2}}{1+[1+(\psi^2\eta/2)]x^2}. \qquad (3.9)$$

A more complicated correlation function, taken from Ref. 24, was also used. In all cases the five parameters I_0, ΔI, ν, η, and r_0 were found. The results of the analysis with the help of these functions are presented in Table II. One can see that these three correlation functions describe the experiment with equal accuracy. It is interesting to note that the description on the basis of the Ornstein-Zernike model also agrees well with the experimental data (see Table II). The discrepancy between the computed and measured intensities $\frac{I_{exp} - I_{theor}}{I_{theor}}$ is illustrated in Fig. 4.

Thus the validity of some particular model of the correlation function cannot be determined based purely on experiment without theoretical justification.

The use of the theoretical values of the indices calculated, based on the three-dimensional Landau-Ginzburg-Wilson model,[25] by the renormalization group method $\eta = 0.0315 \pm 0.0025$, $\nu = 0.630 \pm 0.001$, $\gamma = 1.240 \pm 0.001$, permits describing experiment with the same accuracy of 0.4%, but in this case, as one can see from the differences between the theoretically computed and experimental values of the intensity (Figs. 4(b) and 4(c)), there appears a systematic error. With the use of high-temperature expansions for the three-dimensional Ising model the following values of the indices are obtained[27]:

$$\eta = 0.041 \pm 0.006, \quad \nu = 0.638 \pm 0.002,$$
$$\gamma = 1.250 \pm 0.001.$$

In this case $r_0 = 2.00 \pm 0.03$ Å, while the accuracy of the description of the experiment drops to 1%, and a significant systematic error appears.

The experimental data were also analyzed using correlation functions that include asymptotic corrections to scaling in the form

$$G(x) = G_0(x) + A_1\tau^{\Delta_1}G_1(x), \qquad (3.10)$$

where A_1 is a coefficient that depends on the properties of the system of interest and Δ_1 is a universal index, equal to 1/2.[28]

The function $G_1(x)$ is known exactly only for large and small x, and for the interpolation formula

$$G_1(x) \approx (1+x^2)^{-[2-\eta-(\Delta_1/\nu)]/2} \tag{3.11}$$

is employed. In this method of analysis a sixth, additional parameter A_1 appears. The use of a correlation function of the form (3.8) for G_0 gave results that were practically identical to the data given in the first row of Table II. This convincingly indicates that within the limits of accuracy of this experiment the asymptotic corrections are not significant.

In the analysis with the help of the formula (3.10) and with the use of the indices calculated from the three-dimensional Landau-Ginzburg-Wilson model,[25] the experiment was described with the same accuracy (0.5%), but the systematic error in the differences $(I_{exp} - I_{theor})/I_{theor}$ decreased slightly (compare Figs. 4(b) and 4(e)).

An analogous calculation using the values of η and ν calculated from the high-temperature expansions does not reduce the systematic error, if it is not assumed that the contribution of density fluctuations ΔI to the scattering is anomalously large.

The foregoing analysis thus shows that the values of the critical indices obtained by the renormalization group method best describe the experimental data.

To determine the form of the correlation function the intensity of light scattering not at one, but rather at several scattering angles is also measured. An experiment of this type was performed for scattering angles of 22° 44′ and 132° in a nitrobenzene-*n*-hexane solution[10] in the temperature range $3\cdot10^{-3}$ K $< |T - T_c| < 10$ K. The temperature was maintained constant to within 0.1 mK. A very small cell was employed in order to reduce the role of extinction and multiple scattering. Corrections for extinction and double scattering of light were introduced, for which purpose the formula derived for scattering at 90° was employed.[29] In the analysis of the experimental data the approximation (3.6) and the model function based on the asymptotic expansion (3.5) were employed for the correlation function.[14] The value of the small index was assumed to be known and equal to 0.0315.[25] Both correlation functions describe the experiment with an accuracy of ~2%.

In the more complete experiment the light-scattering functions are measured over a wide range of angles with a small step of 3°–5°. In this formulation of the experiment information about the dependence of the correlation function on the wave number can be obtained at each temperature. From the methodological viewpoint, angular measurements are convenient in that the scattering function is very sensitive to different types of distorting factors and, therefore, the results obtained can be monitored more easily. The small index η in a weakly opalescing solution of nitroethane-*n*-hexane ($T_c = 30.95°$ C, $C_c = 53$ vol. % hexane, $\Delta n = 0.017$) was determined in this manner by Anisimov *et al.*[26,30] A cylindrical cell 4 cm in diameter was employed to increase the reliability of alignment of the optical parts. The measurements were performed in the temperature range $10^{-5} < \tau < 10^{-3}$. In the analysis the correlation function was represented in the form

$$G(k, \tau) = \text{const} \cdot \frac{T}{T_c} \frac{(ck^2 + r_C^2)^{\eta/2}}{k^2 + r_C^2}. \tag{3.12}$$

The parameters η, r_0, and c were found. The value of η was found to equal 0.045 ± 0.010 and $r_0 = 2.4 \pm 0.1$ Å. As regards the coefficient c, the experiment was described with equal accuracy for all values of c in the range $0.1 \leqslant c \leqslant 1$.

Thus a static, critical opalescence experiment makes it possible to find reliably and with high accuracy the values of ν and ρ_0. The problem of determining more accurately the small index η remains unsolved, since the entire complex of optical measurements with the use of data from theoretical calculations indicates the existence of a positive small index, whose values lies in the range from 0.02 to 0.04. This conclusion is also supported by recent neutron scattering measurements,[31] which gave $\eta = 0.039 \pm 0.009$ in the system isobutyl acid (COOD)/D_2O. The analysis was performed using the formula (3.5) for the case $x \gg 1$. The values of r_0 and ν were taken from the light-scattering data.

4. MULTIPLE SCATTERING OF LIGHT

4.1. Double scattering

In the preceding section results referring to purely single scattering of light were presented. In reality, close to the critical point higher order scattering makes an appreciable contribution even in weakly opalescing systems,[2] so that several effective methods for taking multiple scattering into account have now been developed.

One method[32] consists of measuring the intensity of the scattered light in the geometry shown in Fig. 5(a). Here the detector is focused on a point offset from the incident beam by a distance h, rather than on the illuminated volume. Thus light can strike the detector only after a minimum of two scattering processes, and in the process single scattering is completely excluded.

The second method is shown schematically in Fig. 5(b).[23] Here the scattered light is collected from a slit of height H, significantly exceeding the diameter of the incident beam, and the contribution of multiple scattering is thereby increased artificially.

Finally, the third method consists of measuring the depolarization component. This method is applicable only in

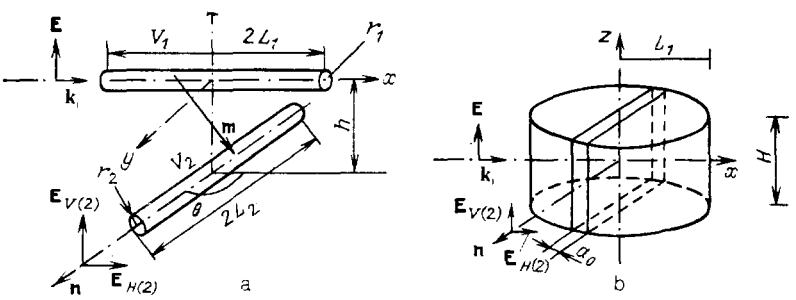

FIG. 5. Geometry of experiment on separating multiple scattering. a) geometry with crossed thin cylinders.[32] b) geometry with a narrow slit of width a_0.[23]

those cases when the order parameter is a scalar quantity, and depolarization is wholly associated with multiple scattering.[33,34]

In all these cases a theoretical calculation for a concrete geometry of the experiment must be performed. Thus far accurate calculations, taken up to the point at which they can be directly compared with experiment, have been performed only for double scattering.

The intensity of the double scattering of light (1.14) taking into account extinction can be written in the form

$$I_\beta^{\alpha(2)} = \frac{I_0}{X^2} R_{sc}^2 \exp\left[-\sigma(L_1+L_2)\right] J_\beta^{\alpha(2)},$$

$$J_V^{V(2)} = \int_{V_1} d\mathbf{r}_1 \int_{V_2} d\mathbf{r}_2 \frac{e^{-\sigma l_0}}{|\mathbf{r}_2-\mathbf{r}_1|^2} (1-m_z^2)^2 G(\mathbf{q}_1) G(\mathbf{q}_2),$$

$$J_H^{V(2)} = \int_{V_1} d\mathbf{r}_1 \int_{V_2} d\mathbf{r}_2 \frac{e^{-\sigma l_0}}{|\mathbf{r}_2-\mathbf{r}_1|^2} m_z^2 [1-m_z^2-(\mathbf{mn})^2] \times G(\mathbf{q}_1) G(\mathbf{q}_2), \quad (4.1)$$

where $J_V^{V(2)}$ is the polarized component and $J_H^{V(2)}$ is the depolarized component, the illuminated volume V_1 is, as a rule, assumed to be a thin cylinder with radius r_1 and length $2L_1$. The volume V_2 is taken to be either a thin cylinder with radius r_1 and length $2L$ [11], or a right-angled parallelepiped of height H and with length $2L$ [33], depending on the formulation of the experiment; and, l_0 is the difference between the lengths of the paths traversed by the singly and doubly scattered light.

The six-fold intergrals, appearing in (4.1), can be substantially simplified in the case when V_1 and V_2 are thin cylinders, and if in so doing the inequalities

$$\sigma r_i \ll 1, \quad r_i \ll L \sin\theta \ (i = 1, 2),$$

where L is the characteristic size of the cell, hold. In real experiments these inequalities are practically always satisfied.

For the geometry of Fig. 5(a) it follows from (4.1) that for weak extinction $\sigma L \ll 1$ and far from the transition point $kr_C \ll 1$ the polarized component is given by[11,29]

$$I_V^{V(2)}(h) = \frac{I_0}{X^2} 2\pi R_{sc}^2 \frac{S_1 S_2}{\sin\theta} \ln\frac{2L\sin\theta}{h}, \quad S_i = \pi r_i^2 \ (i = 1, 2). \quad (4.2)$$

For $h = 0$ in this formula h is replaced by the largest of the radii r_i. For the geometry of Fig. 5(b) this problem was solved in Ref. 23, where the parameter $R^{(2)}$, representing the ratio of the intensity of double-scattering light to the losses of light owing to extinction, was introduced (see the formula (3.7)). The calculation was performed only in the case of weak extinction. In the limit $kr_C \to 0$, for $\theta = 90°$.

$$R^{(2)} = \frac{3H}{8L}\left(\ln\frac{2L}{H} + 0.485\right). \quad (4.3)$$

This formula was used to determine the relative fraction of double scattering in Ref. 7, described in detail in Sec. 3.

The depolarized component $I_H^{V(2)}$ does not have a logarithmic singularity and is virtually constant for small h/L. In lowest order in h/L it has the form

$$I_H^{V(2)}(h) \sim \text{const} - \left(\frac{h}{l}\right)^2.$$

In the case of finite kr_C and appreciable extinction the dependence of $I_\beta^{\alpha(2)}$ on h becomes more complicated, and it can be obtained only by numerical integration. For scattering by 90° this problem was solved in Refs. 23, 29, and 33; the angular dependence of $J_\beta^{\alpha(2)}$ was studied in Refs. 11 and 36. The dependence of both components of double scattering of light on h is shown in Fig. 6. One can see from the figure that the magnitudes of the double scattering $I_V^{V(2)}(h=0)$ can be determined experimentally by at least two methods. One method consists of extrapolating the experimental data on the height dependence $I_V^{V(2)}(h)$ to $h = 0$. The quantity $I_V^{V(2)}(0)$ represents the contribution of double scattering to the total measured intensity. Simple extrapolation is impossible here because of the sharp dependence of $I_V^{V(2)}(h)$ on h for small values of h. The correct procedure is to find the entire curve $I_V^{V(2)}(h)$ by numerical integration, and then to compare it with the experimental data by means of a scale transformation. Curve *1* in Fig. 6 demonstrates the good agreement between the computed and measured values.

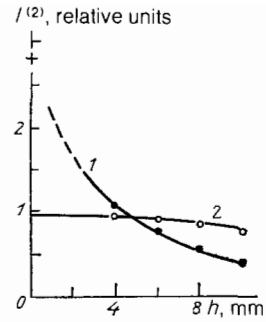

FIG. 6. Components of light scattered at an angle of 90° for the system $\beta\beta'$-dichloroethyl ester–isooctane as a function of height.[11] $kr_C = 0.85$. 1) $I_V^{V(2)}(h)$ 0.1; 2) $I_H^{V(2)}(h)$. The dots are the experimental data, the solid lines show the calculation, and + is the value of $I_V^{V(2)}$ calculated at $h = 0$.

The quantity $I_V^{V(2)}(0)$ can also be found by measuring the depolarized component $I_H^{V(2)}(h)$, which, as one can see from Fig. 6 (curve *2*), is virtually independent of h in a wide range of values of h. To do so, the numerical relationship between $I_V^{V(2)}(0)$ and $I_H^{V(2)}(0)$ must be known. In this procedure the depolarized component $I_H^{V(2)}$ must be measured with high accuracy, since for the aperture ratios employed $I_H^{V(2)}/I_V^{V(2)} \sim 10^{-2}$ (Fig. 7).

In the case of measurements with a slit[23] the degree of depolarization Δ_d depends virtually linearly on the height of the slit H, and according to Refs. 23 and 33 $\Delta_d = (\pi/4) R_{sc} H$. This relation is a consequence of the weak dependence

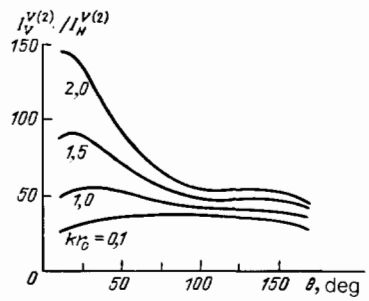

FIG. 7. The computed ratios of the intensities of the components $I_V^{V(2)}(0)/I_H^{V(2)}(0)$ as the function of the scattering angle for different values of kr_C.[11]

of $I_H^{V(2)}$ on h and for this reason is well satisfied in experiments.

4.2. Higher order scattering

Light scattering of order greater than second $I^{(p_i)}$ can appear in weakly opalescing systems. For example, the component $I_V^{V(3)}$ has the form

$$I_V^{V(3)} = \frac{I_0}{X^2} R_{sc}^3 \int_{V_1} d\mathbf{r}_1 \int_{V_K} d\mathbf{r}_K \int_{V_2} d\mathbf{r}_2 \frac{\exp(-\sigma R_{(3)})}{|\mathbf{r}_K - \mathbf{r}_1|^2 |\mathbf{r}_2 - \mathbf{r}_K|^2} \times G(\mathbf{q}_1) G(\mathbf{q}_2) \times G(\mathbf{q}_3) \left[1 - \frac{(\mathbf{r}_K - \mathbf{r}_1)_z^2}{|\mathbf{r}_K - \mathbf{r}_1|^2} - \frac{(\mathbf{r}_2 - \mathbf{r}_K)_z^2}{|\mathbf{r}_2 - \mathbf{r}_K|^2} + \frac{(\mathbf{r}_K - \mathbf{r}_1)_z (\mathbf{r}_2 - \mathbf{r}_c)_z (\mathbf{r}_K - \mathbf{r}_1)(\mathbf{r}_2 - \mathbf{r}_K)}{|\mathbf{r}_K - \mathbf{r}_1|^2 |\mathbf{r}_2 - \mathbf{r}_K|^2} \right]^2, \quad (4.4)$$

where V_c is the volume of the cell and $\mathbf{q}_1$, $\mathbf{q}_2$, and $\mathbf{q}_3$ are the wave vectors after successive reemissions. The calculation of the intensity $I_V^{V(3)}$ is quite a complicated problem even in the simplest approximations. But it should be noted that such a calculation is not desirable, since if $I^{(3)}$ is appreciable, then the parameter in the expansion in terms of the orders of scattering (1.12) is therefore not small. In this case the higher orders $I^{(4)}, I^{(5)}, \ldots$ also start to make a significant contribution to the measured light-scattering intensity. Since it is unrealistic to calculate the sum

$$I^{(p)} = \sum_{i=3}^{\infty} I^{(p_i)}$$

the only method is to determine it experimentally. As follows from the foregoing, the quantity

$$I^{(s)} = I^{(2)} + I^{(p)},$$

can be measured experimentally, for example, from the behavior as a function of the height in the geometry of Fig. 5(a) or from the depolarized scattering. In this case the quantity $I^{(2)}$ found by numerical integration can be subtracted from $I^{(s)}$ and the contribution of scattering of higher orders can thereby be determined. References 15, 16, and 37 are based on these ideas.

In Ref. 37 additional measurements of the depolarized component in a methanol-cyclohexane solution were performed for different distances Δy from the exciting laser beam up to the output window of the cell in order to evaluate the quantity $I^{(p)}$. The intensity $I_H^{V(2)}$ was calculated neglecting extinction. For small values of τ a systematic deviation of the experimental data from the calculations was observed; this deviation was interpreted as a loss of light due to scattering of higher order, primarily triple scattering. The study showed that for $\Delta T > 0.1$ K the quantity $I^{(p)}$ can be neglected, while for a closer temperature $\Delta T = 0.003$ K $I^{(p)}$ was of the order of 15%.

The procedure implemented in Ref. 15 is based on the fact that the formulas for the multiple-scattering intensities of the type (4.4) contain an additional integration over the volume of the cell V_c, which eliminates the logarithmic growth of the component $I_V^{V(3)}$ as $h \to 0$ in the geometry of Fig. 5(a). This result is also valid for higher order scattering. For this reason, the components of scattering of order higher

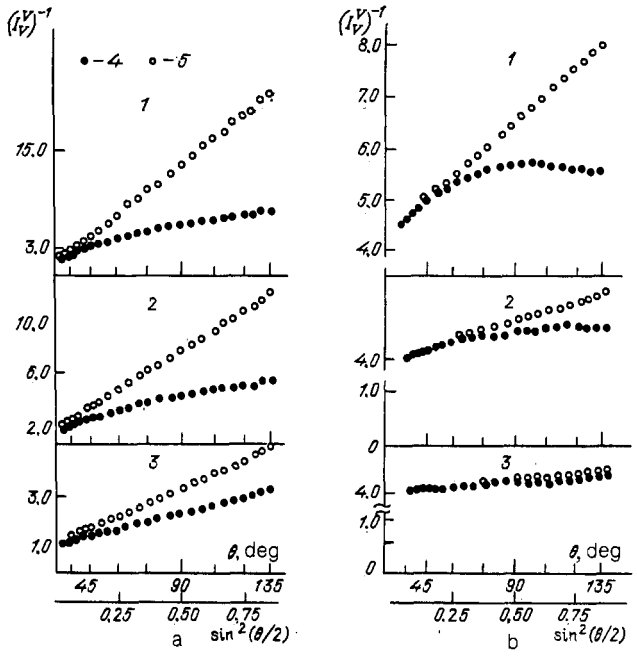

FIG. 8. Angular dependence of the scattered light intensity at different temperatures. a) nitrobenzene-hexane[15]; 1) $\Delta T = 0.014$ K, 2) $\Delta T = 0.024$ Kl; 3) $\Delta T = 0.039$ K, b) BMOAB-isooctane[16]; 1) $\Delta T = 0.145$ K, 2) $\Delta T = 0.405$ K, 3) $\Delta T = 1.5$ K, 4) experiment, 5) single scattering separated.

than second are smooth functions of h for small values of h. The theoretically computed double scattering component I_V^V, exp(h) was subtracted from the measured height data $I_V^{V(2)}(h)$. The magnitude of the multiple scattering $I_V^{V(p)}$ was obtained by extrapolating the difference $I_{V,\exp}^V(h) - I_V^{V(2)}(h)$ to $h = 0$. The experimental data on the intensity of scattered light in the nitrobenzene-hexane system were analyzed by this method. Angular measurements were performed in a cylindrical cell 3 cm in diameter for different values of $T - T_c$. It should be noted that in this experiment $I_V^{V(p)}$ plays an appreciable role starting with $\Delta T \sim 0.05$ K and reaches 40% for $\Delta T \sim 0.015$ K, which is two times greater than the contribution of double scattering. This method enabled the determination of the critical indices and the scattering constant with adequate accuracy for this strongly opalescing system: $\nu = 0.62 \pm 0.02$, $\gamma = 1.21 \pm 0.02$, $r_0 = 2.7 \pm 0.2$ Å, $B = 0.29 \pm 0.02$, cm^{-1}. The analysis was performed by the iteration method; the parameters found from measurements of the scattering function far from the critical point, of the type of the curve *3* in Fig. 8, were employed as the zeroth-order approximation.

There exist systems for which the scattering constant is so large that the contribution of multiple scattering is not small even far from the critical point. In this case it is impossible to describe the critical parameters in the zeroth-order approximation from the light-scattering intensity. The fundamental possibility of studying such systems by optical methods was demonstrated in Ref. 16, where a segregating solution of isooctane-BMOAB with the refractive indices of the components of the mixture differing by $\Delta n = 0.25$, where BMOAB is a nematic liquid crystal, was studied. The experimental scattering functions for the system are shown in Fig. 8(b). One can see that the light-scattering intensity is anomalously high at large angles θ; this is explained by the

TABLE III. Critical parameters found from different types of experiments.[15]

Type of experiment	ν	r_0, Å	B, cm^{-1}
Measurements of transmitted light intensity	0.60±0.03	3.4±0.4	1.15±0.30
Measurement of the angular dependence of the scattered light intensity	0.60±0.04	3.9±1.0	—
Combined analysis of data on attenuation and scattering of light	0.63±0.01	3.2±0.2	0.95±0.04

presence of multiple scattering, for which the scattering function is much more nearly circular than for single scattering.[2,15]

In the analysis of the experimental data the critical parameters obtained from measurements of the temperature dependence of the extinction coefficient were employed as the zeroth-order approximation. With their help the single scattering was separated and the values of B, r_0, and ν were found (Table III). Even after several iteration steps the spread in these parameters is still quite high. This is most likely attributable to the limited temperature range studied, since the relative fraction of multiple scattering equals about 50% of the total intensity already for $\Delta T = 0.15$ K.

The accuracy can be substantially increased by taking into account the fact that the data on extinction and on the scattering functions contain mutually complementary information on the values of the parameters.

Figure 9 shows the regions of admissible values of the parameters for each experiment. One can see that these regions are strongly elongated intersecting troughs. The region of intersection of the troughs corresponds to the values of the parameters that best describe both experiments simultaneously. Since this region is much smaller than for each experiment separately, combined analysis substantially reduces the variances of the critical parameters determined. The results are given in Table III.

Thus the methods developed for taking into account multiple scattering enable significant expansion of the classes of systems admissible for precision measurements. This analysis, as we can see, always requires additional experiments and numerical calculations. The Ornstein-Zernike approximation is fully adequate for calculating multiple scattering with the present accuracy of experiments.

5. STUDY OF THE KINETIC PROPERTIES IN THE CRITICAL REGION

The measurement of the spectral composition of scattered light and of the time correlation function near the critical points enables the study of the kinetics of the order parameter, the spectra of hydrodynamic motions, and

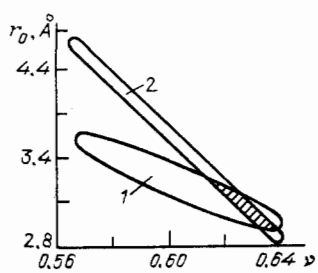

FIG. 9. Confidence regions of values of the parameters r_0 and ν for the system BMOAB-isooctane.[16] 1) extinction experiment; 2) light scattering experiment.

relaxation processes. The characteristic rates of these processes cover a very wide range of frequencies from 10^1 up to 10^{11} Hz, and the most diverse methods are now employed to record them.

5.1. Kinetics of fluctuations of the order parameter

We shall study first the dynamic properties of the order parameter. The spectrum of the scattered light is determined by the time correlation function

$$\langle C_{\mathbf{q}}(t)\, C_{-\mathbf{q}}(0)\rangle = \langle |C_{\mathbf{q}}|^2\rangle\, e^{-\Gamma t}, \tag{5.1}$$

where $\Gamma = D(q)q^2$ is the decay constant and $D(q)$ is the temperature- and wave-vector-dependent thermal diffusivity near the critical point of the liquid-vapor and the coefficient of diffusion near the segregation point. The coefficient D vanishes in the limit $\mathbf{q}\to 0$ at the critical point. This phenomenon is known as the critical suppression of fluctuations. The characteristic frequencies of the fluctuations of the order parameter usually fall into the band from tens of hertz to several kilohertz, and are studied by the methods of correlation spectroscopy.

Measurements of the time correlation function at different scattering angles and temperatures enable the study of the dependence of the coefficient D on the temperature and wave number since $q = 2k\sin(\theta/2)$. The typical dependence of D on kr_C is shown in Fig. 10.

In the theory of critical phenomena the coefficient D is related with the coefficient of shear viscosity η_s and satisfies the asymptotic equation[39]

$$D = \overline{D} + \frac{k_B T}{6\pi\eta_s r_C}\,\Omega(qr_C), \tag{5.2}$$

where $\overline{D}$ is the regular part of D. The coefficient η_s can be represented in an analogous form[39]:

$$\eta_s = \overline{\eta}_s + r_C^{x_\eta} E(qr_C). \tag{5.3}$$

The regular part $\overline{\eta}_s$ in (5.3) is described by the empirical law

$$\overline{\eta}_s = A_\eta \exp B_\eta/k_B T,$$

where A_η and B_η are adjustable parameters, and x_η is the dynamic index. It was proposed in Ref. 39 that η_s be represented in the form

$$\eta_s = \overline{\eta}_s (Q_0 r_C)^{x_\eta}, \tag{5.4}$$

where Q_0 is a system-dependent amplitude, for analysis of experimental data on the viscosity at $q = 0$.

The dynamic scaling function $\Omega(qr_C)$ is known exactly in two limiting cases

$$\begin{aligned}\Omega(qr_C) &= R \quad \text{for} \quad qr_C = 0,\\ &= (qr_C)^{1+x_\eta} \quad \text{for} \quad qr_C \gg 1;\end{aligned} \tag{5.5}$$

here R is a universal constant.

The complete form of the function $\Omega(qr_C)$ was calculated by Kawasaki[40,41] by the method of interacting modes. With the use of the Ornstein-Zernike approximation

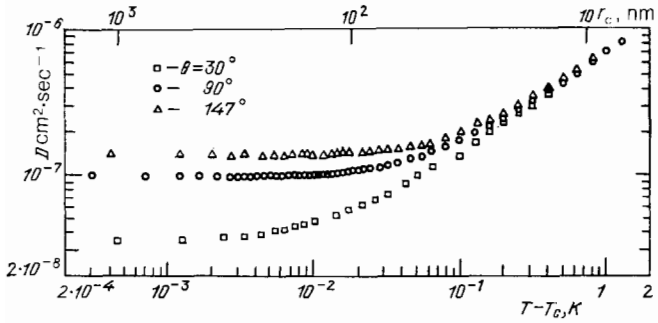

FIG. 10. Temperature dependence of the coefficient of diffusion $D(q)$ in the mixture 3-methyl pentane-nitroethane for three scattering angles.[38]

$$\Omega(y) = \frac{3}{4y^2}\left[1 + y^2 + (y^3 - y^{-1})\operatorname{arctg} y\right]. \tag{5.6}$$

In this approximation $\Omega(0) = 1$ and $\Omega = (3\pi/8)y$ for $y \gg 1$. An analogous calculation for the shear viscosity gives

$$\eta_s = \bar{\eta}_s\left[1 + \frac{8}{15\pi^2}\ln(q_m r_c)\right]. \tag{5.7}$$

These results are also obtained by the method of separation of the contributions of collective variables.[42]

It follows from the formulas (5.1), (5.2), and (5.5) that the decay constant has the form

$$\Gamma = q^z g(qr_c), \tag{5.8}$$

where $z = 3 + x_\eta$ and

$$\begin{aligned} g(qr_c) &\sim (qr_c)^{-1-x_\eta} \quad \text{as} \quad qr_c \to 0, \\ &\sim \text{const} \quad \text{as} \quad qr_c \to \infty. \end{aligned} \tag{5.9}$$

The value of the dynamic index $x_\eta = 0.054$ was obtained from the exact solution of Kawasaki's equation in Refs. 43 and 44 with the small index $\eta = 0$. It follows from the renormalization group in the approximation[45] quadratic in ε that $x_\eta = 0.065$. The universal constant R also does not have a unique value: the method of interacting modes gives $R = 1.03$,[46] the renormalization group method gives $R = 1.2$,[45] while subsequent refinement gave the value $R = 1.07$.[47]

Experimental studies confirm the theoretically predicted character of the behavior of the coefficients D and η_s in the critical region. In the last few years the main attention in the analysis of experimental data has been devoted to two limiting temperature regions—far from and adjacent to the critical point, since the exact solution for D, as follows from (5.2) and (5.5), is known only for these cases.

To determine the index x_η over a wide temperature range, measurements of the decay constant Γ for different scattering angles, i.e., different values of q, are being performed. Since at a finite distance from T_c the function $g(kr_c)$ in (5.9) is unknown, it is assumed that Γ depends on q in a power-law fashion $\Gamma \sim q^{z_{\text{eff}}}$ where the exponent z_{eff} depends on $(T - T_c)$. To obtain the value of $z = 3 + x_\eta$, z must be extrapolated to the critical point itself. Two methods of extrapolation in τ and r_c, giving somewhat different values of z, are possible. For the system consisting of 3-methyl pentane-isooctane for temperature extrapolation ($\tau \to 0$) $z = 3.063 \pm 0.024$ and $z = 3.054 \pm 0.024$ for extrapolation with respect to the correlation radius ($r_c^{-2} \to 0$).[38,48] Without extrapolation the maximum value for z for this system is $z = 2.99 \pm 0.05$,[49] which is close to the value $z = 2.992 \pm 0.014$ in Ref. 50. Similar results are also obtained in the system polydimethyl siloxane—diethyl carbonate: $z = 3.04 \pm 0.03$.[51]

The index x_η, according to (5.3), can also be determined from the temperature dependence of the shear viscosity. For the solution 3-methyl pentane-nitroethane the values $x_\eta = 0.063 \pm 0.002$ and $Q_0 = 1.4 \pm 0.9$ nm^{-1} were obtained in Refs. 52–54. A more detailed analysis of the data from these studies[38] gave the more accurate value $x_\eta = 0.062 \pm 0.005$. Investigations of water solutions of isobutyl acid[55] gave the value $x_\eta = 0.063 \pm 0.004$ for the critical isochore and $x_\eta = 0.057 \pm 0.006$ along the coexistence curve.

As we can see, the accuracy with which x_η is determined here is higher than in optical measurements, though in this case data on light scattering are also necessary, since the correlation radius appears in the expression for η_s.

The experimental data on the decay constant far from the critical point are employed to find the universal parameter R, as follows from (5.2) and (5.5). In so doing the contribution of the regular part $\bar{D}$ varies from 0.1 to 2% depending on the value of τ.[38] In all experiments the values of R were greater than 1, and clustered around $R = 1.01$–1.02 with an error of the order of 4–6%.[10,38,55–57] The value $R = 1.06 \pm 0.04$, obtained in the recent paper of Ref. 55 for a water solution of isobutyl acid, is special.

Thus quantitative agreement between the theoretical calculations and the experimental results is obtained for the dynamic index x_η, though the experimental data do not permit determining which method for calculating the critical index is most reliable.

Similar agreement is not obtained for the universal constant R, and the large error with which it is determined is apparently associated with the uncertainty in the value of r_c.

The foregoing analysis was based on the assumption that the time correlation function

$$f^{(1)}(t) = \langle C_{\mathbf{q}}(t) C_{-\mathbf{q}}(0)\rangle$$

is purely exponential and the decay constant Γ is described by the system of equations (5.2) and (5.3). It was shown in Ref. 58 that taking into account the temporal dispersion of the coefficient of shear viscosity causes $f^{(1)}(t)$ to deviate from an exponential law. This behavior was observed experimentally in Refs. 59 and 60 in the system 3-methyl pentane-nitroethane. The logarithm of the function $f^{(1)}(t)$ was represented in the form

$$\ln f^{(1)}(t) = \text{const} - K_1 t + \frac{1}{2}K_2 t^2, \tag{5.10}$$

and in addition the ratio of the coefficients K_2/K_1^2 increases as $T \to T_c$, and for $\Delta T = 0.0018°$ K equals 0.033 ± 0.008, which agrees with the theoretical predictions.[58]

Just as in the case of the investigations of the integrated characteristics of the scattered light, the main distorting factor in the determination of the dynamic critical parameters is the multiple scattering of light.

The experimental determination of the spectra or time correlation function is quite a complicated and lengthy procedure. For this reason, up to now the multiple-scattering spectra have not been studied as fully as the integrated intensity. It is precisely for this reason, as one can see from the foregoing analysis, that the main, reliable results on the dynamic critical parameters z, x_η, and R were actually ob-

tained only for the binary mixture 3-methyl pentane-nitroethane. For this solution, it follows from measurements of the integrated intensity[7] that the corrections for multiple scattering do not exceed several percent (see Sec. 3), even very close to T_c, and therefore the effect of this distorting factor on the spectra and time correlation function is very small.

In the analysis of the multiple-scattering spectrum it is of greatest interest to determine how its form differs from that of the single-scattering spectrum. These features can be easily illustrated for the example of the normalized correlation function of double scattering $f^{(2)}(t)$ in the geometry of the experiment shown in Fig. 5(a) with $h = 0$. For the polarized component of the scattered light, using the Ornstein-Zernike approximation,[61] we obtain

$$\tilde{f}^{(2)}(t) = \frac{b(t)}{b(0)}, \qquad (5.11)$$

where

$$b(t) = \int_0^{L\sin\theta/r_1} d\rho\,[(\rho^2+1)^{1/2}-\rho] \times \int_0^{2\pi} d\varphi' \frac{\exp\{\sigma r_2 \rho[\operatorname{tg}(\theta/2)\sin\varphi' + \cos\varphi' - 1]\}}{[1-\alpha\cos(\varphi'-\theta)](1-\alpha\cos\varphi')} \times \exp[-t(\Gamma(q_1)+\Gamma(q_2))]; \qquad (5.12)$$

here φ' is the angle of one of the reemissions, and $(\alpha = 2(kr_c)^2[1+2(kr_c)^2]^{-1}$. As the critical point is approached ($\alpha \to 1$) three regions of angles φ' making the main contribution to the integral (5.12) can be distinguished: $\varphi' \sim \theta, \varphi' = 0, \varphi' = \theta/2$. Since near T_c the scattering function is extremely strongly elongated in the forward direction, the probability of double scattering in which one of the scattering events occurs at zero angle ($\mathbf{q}_1$ or $\mathbf{q}_2$ equals 0) while the other occurs at the single-scattering angle increases rapidly. The spectrum of such double scattering is similar to the single-scattering spectrum, and its contribution to (5.12) is quite large, since it corresponds to the regions $\varphi' \sim \theta, \varphi' \sim 0$. This case was discussed in detail in Ref. 62 under the assumption that there is no extinction, $\sigma = 0$. Taking extinction into account leads to the appearance of a third region of angles near $\varphi' \sim \theta/2$, which corresponds to the contribution of rays traversing the shortest path in the medium. The spectrum of this contribution is different from the single-scattering spectrum.

In the general case the form of the time correlation function or the spectrum of the central component can be calculated only numerically. Calculations using formulas of the type (5.12) show that the time correlation function is not

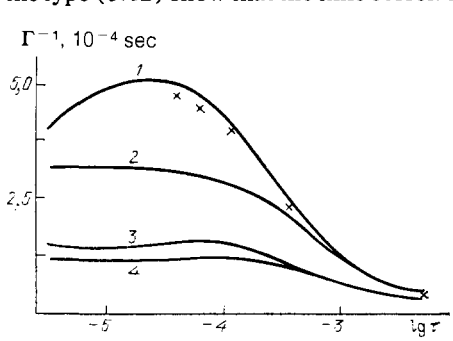

FIG. 11. Computed temperature dependence of the half-width of the light scattering contour.[61] 1) $I_V^{V(2)}$, $\theta = 90°$, ×—experiment[63]; 2) $I_V^{V(1)}$, $\theta = 90°$, 3) $I_V^{V(2)}$, $\theta = 150°$, 4) I_V^{V}, $\theta = 150°$.

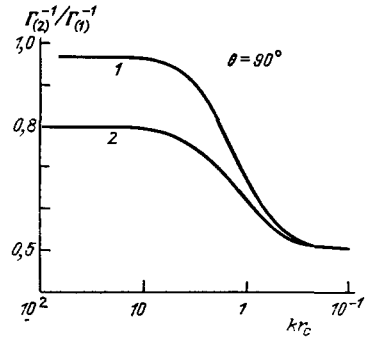

FIG. 12. Ratio of the correlation times of double scattering of light $\Gamma_{(2)}^{-1}$ to the single-scattering time $\Gamma_{(1)}^{-1}$ in the "spherical" geometry as a function of kr_C in the system methanol-cyclohexane.[59] 1) polarized component $I_V^{V(2)}$, 2) depolarized component $I_H^{V(2)}$.

exponential and decays somewhat more slowly than in the case of single scattering. The half-width of the computed spectra is presented in Fig. 11, which also shows the results of experimental studies[63] of the spectrum of the central component of double scattering in the nitrobenzene-hexane system. The experimental data on the half-width were obtained in the geometry of Fig. 6(a) for small values of h.

It is interesting to note that the ratio of the half-widths of single $\Gamma^{(1)}$ and double $\Gamma^{(2)}$ scattering depends on the geometry of the experiment. Thus, in Ref. 49, for measurements in wide beams $r_1 = 5$ mm using very small detecting diaphragms (so-called spherical geometry) the reverse inequality $\Gamma^{(2)} > \Gamma^{(1)}$ holds (Fig. 12).

A correct analysis of the spectra, as done for the integrated intensity, has not yet been performed, and spectra of order higher than second have not been studied.

5.2. Spectrum of the Mandel'shtam-Brillouin doublet

One method for studying the kinetics of critical fluctuations is ultrasonic spectroscopy.[64] Such measurements are usually performed up to frequencies of the order of several hundreds of megahertz. At higher frequencies Mandel'shtam-Brillouin spectroscopy, which in principle gives information about the high-frequency behavior of sound, is employed. We shall examine the spectral intensity of the components of the Mandel'shtam-Brillouin doublet in segregating solutions:

$$I_{V\rho}^{V(1)}(\omega) = \frac{I_0 V R_{sc}(\rho)}{2\pi X^2} \times e^{-\sigma l}\left[\frac{\Gamma_{MB}q^2}{(\omega-vq)^2+\Gamma_{MB}^2q^4} + \frac{\Gamma_{MB}^2q^2}{(\omega+vq)^2+\Gamma_{MB}^2q^4}\right], \qquad (5.13)$$

where $R_{sc}(\rho)$ is a constant characterizing the scattering by adiabatic fluctuations of the density, $\Gamma_{MB} = \mathrm{Re}[(4/3)\times\eta_s + \eta_v]/2\rho$, η_v is the coefficient of bulk viscosity, and v is the velocity of sound. The values of the velocity of sound and the coefficients of viscosity appearing in the formula (5.13) are the high-frequency values, since in the entire range of scattering angles θ the frequency of the components of the doublet $\Omega_{MB} = vq$ is much higher than ω_C—the characteristic frequency of concentration fluctuations. At the same time, the critical contribution to the complex coefficient of bulk viscosity has the form[65,66]

$$\Delta\eta_V(\Omega_{MB}) = \frac{b_1 + ib_2}{\Omega_{MB}}, \qquad (5.14)$$

where b_1 and b_2 are constants determining the high-frequen-

cy behavior of sound. The analogous contribution of the coefficient of shear viscosity is small[58,64] and is usually ignored. In this case the velocity of sound at the frequency Ω_{MB} and the half-widths of the components of the doublet $\delta\Omega_{MB}$ equal

$$v^2(\Omega_{MB}) = v_0^2 + \frac{\Omega_{MB}}{\rho}\,\mathrm{Im}\,\eta^{reg}(\Omega_{MB}) + \frac{b_2}{\rho}, \qquad (5.15)$$

$$\delta\Omega_{MB} = \Gamma_{MB}q^2 = \frac{q^2}{2\rho}\,\mathrm{Re}\,\eta^{reg}(\Omega_{MB}) + \frac{b_1 q}{2\rho v(\Omega_{MB})}, \qquad (5.16)$$

where $\eta^{reg}(\Omega_{MB})(4/3)\eta_s^{reg}(\Omega_{MB}) + \eta_v^{reg}$ (Ω_{MB}), and $\eta_v^{reg}(\Omega_{MB})$ and $\eta_s^{reg}(\Omega_{MB})$ are the regular parts of the coefficients of bulk and shear viscosity.

It follows from the formulas (5.15) and (5.16) that neither the velocity of sound nor the half-width of the components of the doublet depend on the closeness to T_c; this is confirmed experimentally.[67,68] The parameters b_1 and b_2 can in principle be found from the dependence of v and $\Delta\Omega_{MB}$ on the scattering angle, i.e., on q. In this case the formula (5.15) permits determining, from the known v and Ω_{MB}, the dispersion $\eta^{reg}(\Omega_{MB})$ and the sum $v_0^2 + (b_2/\rho)$. To analyze $\delta\Omega_{MB}$ it is convenient to separate its dependence on the scattering angle in an explicit form:

$$\delta\Omega_{MB} = \frac{2k^2}{\rho}\,\mathrm{Re}\,\eta^{reg}\sin^2\frac{\theta}{2} + \frac{kb_1}{\rho v}\sin\frac{\theta}{2}. \qquad (5.17)$$

For a system of the nitroethane-isooctane type[67,69] ($kb_1/\rho v \sim 3\cdot10^7\,\mathrm{sec}^{-1}$, $(2k^2/\rho)^2 \times \mathrm{Re}[(4/3)\eta_s^{reg} + \eta_v^{reg} \sim 1.2\cdot10^9\,\mathrm{sec}^{-1}$) at angles of the order of 90° the critical contribution to the half-width equals about 3%, but for small angles it grows rapidly and, for example, at an angle $\theta \sim 5°$ it equals about 35%.

Thus in studying the components of the doublet the measurements at small angles should give the most important information about the critical behavior of the system.[70]

In such measurements the contribution of double scattering $I^{(2)}_{(\rho,C)}(\omega)$, where one component is due to scattering by concentration fluctuations and the other is due to scattering by adiabatic fluctuations of the density, could be a distorting factor. A general analysis of the spectral composition of doubly scattered light was performed in Ref. 2, while a concrete calculation for the geometry of Fig. 5(a) was performed in Ref. 70 for two solutions: weakly opalescent nitroethane-isooctane and strongly opalescing nitrobenzene-hexane. It turned out that the integrated scattering intensity $I^{V(2)}_{V(\rho,C)}$ is small for the weakly opalescing system because of the smallness of the scattering constant of this system, and even for $kr_C \sim 40$ it equals only 1.5% of the integrated intensity $I^{V(1)}_{V(\rho)}$. Its position is virtually identical to the frequency Ω_{MB}, since for such values of kr_C there is a high probability that one of the reemission events occurs at zero angle.

In a strongly opalescing system the situation changes somewhat because of the existence of significant extinction and, therefore, the weight of the rays traversing the shortest path in the medium is relatively high, analogously to the situation with the central component. As a result, the contour of $I^{V(2)}_{V(\rho,C)}$ has a maximum at frequencies $\Omega < \Omega_{MB}$. For this reason the experimentally obtained contour of the Mandel'shtam-Brillouin component $I^{V}_{V\ MB}$ $I^{V(1)}_{V(\rho)} + I^{V(2)}_{V(\rho,C)}$ lies somewhat closer to the undisplaced line, and neglecting $I^{V(2)}_{V(\rho,C)}$ the experiment can be interpreted as a drop in the velocity of sound as T_c is approached and therefore as the presence of a negative dispersion. In addition, when $I^{V(2)}_{V(\rho,C)}$ is neglected the value obtained for the absorption coefficient is too high, since the half-width of the contour $I^{V(2)}_{V(\rho,C)}$ is greater than the half-width of $I^{V(1)}_{V(\rho)}$ for both strongly and weakly opalescing systems.

Multiple scattering of light is also observed in the low-frequency part of the wing of the Rayleigh line (WRL), which arises owing to scattering by fluctuations of the tensor anisotropy parameter $\hat{\zeta}$. Since the characteristic frequencies of fluctuations of $\hat{\zeta}$ are several orders of magnitude higher than the characteristic frequencies of concentration fluctuations, a narrow, strong line $I^{V(2)}_{H} + I^{V(p)}_{H}$, which is superposed on the WRL and thereby distorts its shape, appears in the spectrum of the I^{V}_{H} component.[5,32]

The ratio of the integrated intensities of multiple concentration scattering $I^{V(2)}_{H} + I^{V(p)}_{H}$ and of the wing $I^{V(1)}_{H(\zeta)}$ depends strongly on the closeness to the critical point and the geometry of the experiment. Thus for the nitrobenzene-hexane mixture in the geometry of Ref. 15 the ratio $(I^{V(2)}_{H} + I^{V(p)}_{H})/I^{V(1)}_{H(\zeta)}$ varies from 0.1 for $kr_C \sim 0.2$ up to 30 for $kr_C \sim 1$. For spectral measurements this ratio is one to two orders of magnitude higher because of the fact that large apertures must be used for the scattered light, i.e., multiple scattering must be taken into account in the entire critical region when determining the parameters of the WRL.

In Ref. 71 in a study of the spectrum of the WRL in the same mixture the intensity of the component $I^{V}_{H(\zeta)}$ was observed to grow as T_c was approached. One reason for the anomalous growth in the intensity could be multiple scattering, in which one scattering component is due to scattering by fluctuations of $\hat{\zeta}$ while the others are due to scattering by concentration fluctuations, analogously to $I^{(2)}_{(\rho,C)}$. In the double-scattering approximation the component $I^{V(2)}_{H(C,\zeta)}$ in the geometry of Fig. 5(a) for $h = 0$ has the form[72]

$$I^{V(2)}_{H(C,\zeta)} = A\tau^{-\gamma_*}\frac{2\pi^3(1-\alpha)}{\alpha^2}\left[\frac{1+\alpha^2}{(1-\alpha^2)^{1/2}} - 1\right] r_1^2 r_2^2 \ln\frac{2L}{r_2}, \qquad (5.18)$$

where $A = I_0 R_{sc} R_{sc}(\zeta)/X^2$, and $R_{sc}(\zeta)$ is the scattering constant characterizing the scattering by fluctuations of $\hat{\zeta}$. The formula (5.18) was obtained with logarithmic accuracy with respect to the small parameter r_2/L.

Because of the lack of information on the geometry of the experiment it is impossible to make a quantitative analysis of the data of Ref. 72 under the assumption that the intensity of WRL can be represented in the form $I^{V(1)}_{H(\zeta)} + I^{V(2)}_{H(C,\zeta)}$. To evaluate the contribution of $I^{V(2)}_{H(C,\zeta)}$ we shall employ the geometry of Ref. 15. It follows from the formula (5.18) that the intensities $I^{V(1)}_{H(\zeta)}$ and $I^{V(2)}_{H(C,\zeta)}$ are comparable for $kr_C \sim 1$, i.e., the observed intensity of WRL is doubled and therefore this form of scattering is not small in the critical region.

6. LIGHT SCATTERING IN NEMATIC LIQUID CRYSTALS

Thus far we have been studying systems in which critical opalescence arises owing to scattering of light by fluctuations of a scalar order parameter. There exists a large class of liquids consisting of strongly elongated molecules, which are capable of forming a liquid-crystalline state. To describe critical phenomena in such systems a tensor order parameter must be introduced. In the liquid-crystalline state a large number of different mesophases,[73] transitions between which are diverse in nature and can be both first- and second-order phase transitions, is observed. The transition

from the isotropic phase to the liquid-crystalline phase, which has been studied in greatest detail both theoretically and experimentally, is especially strongly manifested in experiments on light scattering.

6.1. Isotropic-phase—nematic phase transition

Here we shall study the simplest phase transition from the isotropic liquid into a nematic liquid crystal (I-N), which is a first-order phase transition close to a second-order transition, since the heat of fusion in it is very small (~ 1 J/cm^3). This transition is usually described by an effective Hamiltonian H within the framework of the Landau–de Gennes model[74–76]

$$H = \int \mathrm{d}\mathbf{r} \Big[a\tau \operatorname{Sp} \hat{S}^2 - \frac{1}{2} L_1 \operatorname{Sp} (\hat{S}\Delta\hat{S}) + \frac{1}{2} L_2 \operatorname{Sp} (\nabla\hat{S})^2 - \frac{1}{3} B \operatorname{Sp} \hat{S}^3 + \frac{1}{4} C (\operatorname{Sp} \hat{S}^2)^2 + \frac{1}{5} E \operatorname{Sp} \hat{S}^2 \operatorname{Sp} \hat{S}^3 + \frac{1}{6} D_1 (\operatorname{Sp} \hat{S}^2)^3 + \frac{1}{6} D_2 (\operatorname{Sp} \hat{S}^3)^2 \Big], \tag{6.1}$$

where $\tau = (T - T^*)/T^*$ and $S_{\alpha\beta}$ is the tensor order parameter, which is an asymmetric tensor with zero trace. This parameter can be determined in terms of any physical quantity with the same tensorial dimension, for example, the magnetic susceptibility, the dielectric permittivity, etc. In light scattering experiments it is convenient to interpret $S_{\alpha\beta}$ as the traceless part of the dielectric permittivity tensor $\varepsilon_{\alpha\beta}$ at an optical frequency. The intensity of single scattering of light by fluctuations of $\varepsilon_{\alpha\beta}$ in the isotropic phase has the form

$$I_{\mathrm{V}}^{\mathrm{V}} = \frac{2}{3} \frac{I_0 V R_{\mathrm{sc}}}{x^2} G_{\mathrm{V}}^{\mathrm{V}}(q)\, e^{-\sigma l}, \tag{6.2}$$

$$I_{\mathrm{H}}^{\mathrm{V}} = \frac{1}{2} \frac{I_0 V R_{\mathrm{sc}}}{x^2} G_{\mathrm{H}}^{\mathrm{V}}(q)\, e^{-\sigma l}, \tag{6.3}$$

where

$$G_{\mathrm{V}}^{\mathrm{V}}(0) = G_{\mathrm{H}}^{\mathrm{V}}(0) = 1, \quad R_{\mathrm{sc}} = \frac{\pi^2}{5\lambda^4} \langle \operatorname{Sp} \delta\hat{\varepsilon}^2 \rangle. \tag{6.4}$$

In the Gaussian approximation, using (6.1), we obtain[76,77]

$$G_{\mathrm{V}}^{\mathrm{V}}(q) = \frac{1}{4} \left(\frac{3}{1+q^2 r_{\mathrm{C1}}^2} + \frac{1}{1+q^2 r_{\mathrm{C2}}^2} \right),$$
$$G_{\mathrm{H}}^{\mathrm{V}}(q) = \frac{1}{2} \left(\frac{1-\cos\theta}{1+q^2 r_{\mathrm{C1}}^2} + \frac{1+\cos\theta}{1+q^2 r_{\mathrm{C3}}^2} \right). \tag{6.5}$$

The correlation radii r_{C1}, r_{C2}, and r_{C3} have the same temperature dependence and are interrelated by the expression

$$4r_{\mathrm{C3}}^2 = r_{\mathrm{C1}}^2 + 3r_{\mathrm{C2}}^2.$$

In this approximation

$$R_{\mathrm{sc}} = \frac{\pi^2}{\lambda^4} k_{\mathrm{B}} T \chi(\tau), \tag{6.6}$$

where the susceptibility is $\chi(\tau) = (a\tau)^{-1}$.

Thus it follows from the formulas (6.2)–(6.6) that as the temperature is lowered and T^* is approached the intensity of the scattered light of both polarizations must increase and at the same time the form of the scattering function must change. In reality, the temperature T^* is not attainable, since before this temperature is reached a first-order phase transition occurs at T_{c}.

The increase in the intensity of light scattering has been observed experimentally in MBBA liquid crystals.[78–80] Neglecting the immediate neighborhood of T_{c}, in a wide range of temperatures $\Delta T = T - T_{\mathrm{c}} \sim 20$ K the inverse intensity is a linear function of the temperature (Fig. 13). Approximation of the experimental dependence by a straight line gives $T_{\mathrm{c}} - T^* \sim 1.6$ K. The quite large difference $T_{\mathrm{c}} - T^*$ limits the radii R_{Ci}, $i = 1$, 2, and 3. For this reason the asymmetry of the angular dependence of light scattering must be small. The correlation radius was determined in Ref. 80, where the intensity of the scattered light was measured to within 0.1% at two fixed scattering angles. The maximum angular asymmetry in the immediate neighborhood of T_{c} equalled 1%, which corresponded to a correlation radius $r_{\mathrm{C}} \approx 100$ Å with $r_0 = 5.5 \pm 0.3$ Å. Such a small asymmetry makes it impossible to distinguish the correlation radii r_{Ci} experimentally and therefore the description is given in the approximation of one correlation radius, which corresponds to $L_2 = 0$ in (6.1).

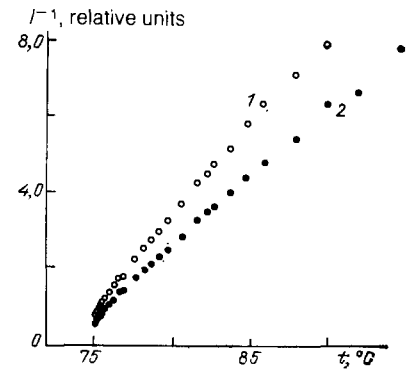

FIG. 13. Temperature dependence of the inverse light-scattering intensity in the isotropic phase of BMOAB at an angle of 90°.[80] 1) the component $I_{\mathrm{V}}^{\mathrm{V}}$; 2) the component $I_{\mathrm{H}}^{\mathrm{V}}$.

In the immediate vicinity of T_{c} the character of the temperature dependence of the light-scattering intensity changes, and it starts to grow more rapidly with the temperature.[79] This phenomenon was analyzed in detail in Ref. 81 for BMOAB liquid crystals, in which the region of existence of the nematic phase is very wide and the smectic phase is absent.

The intensities of both components of the scattered light were measured at an angle of 90°, as was the intensity of the liqht passing through the cell I_{tr}. The accuracy of the measurements equalled 0.7%. Since the scattering function is practically circular ($kr_{\mathrm{C}} \ll 1$), these data make it possible to determine the absolute scattering constant. Indeed, in this case

$$I_{\mathrm{scatt}} = I_0 \frac{V R_{\mathrm{sc}}}{X^2} e^{-\sigma l},$$
$$I_{\mathrm{trans}} = I_{\mathrm{trans}(0)}\, e^{-\sigma l_{\mathrm{trans}}}, \tag{6.7}$$

where $\sigma = (40\pi/9) R_{\mathrm{sc}}$.[81] The quantity $R_{\mathrm{sc}}(\tau)$ was determined in absolute units with adequate accuracy from the system (6.7) by the method of least squares. It varies in the temperature range $0 < T - T_{\mathrm{c}} < 20$ K from 10^{-3} cm^{-1} up to $2 \cdot 10^{-2}$ cm^{-1}. With such a large value of R_{sc} the contribution of higher order scattering can be appreciable.

The intensity of light double-scattered by fluctuations of the tensor order parameter was calculated as a function of

h for the geometry of Fig. 5(a). The experimental measurements and analysis with the help of the formulas derived enabled estimation of the magnitude of the double scattering. Even for $T \sim T_c$ it did not exceed 3%. This means that the deviation from linearity in Fig. 13, which reaches a maximum value of about 30%, cannot be explained by higher order scattering.

Therefore the nonuniversality of the behavior of the light scattering intensity must have a physical nature. It is natural to conjecture that far from T_c the system is described by Landau's classical theory, while near T_c a transition occurs into the fluctuation region, where the contribution to the susceptibility owing to the interaction of fluctuations of the order parameter becomes important.[82]

The experimental data were interpreted with the help of calculations performed on the basis of perturbation theory. The justification for this was the small deviation of the temperature dependence of the inverse susceptibility χ^{-1} from a linear dependence. In the calculation of the fluctuation corrections the integrals over the wave numbers were cut off at a limiting wave number q_m in order to avoid divergences in the diagrams of the perturbation series. In Refs. 82 and 83 q_m appeared as a parameter in the final expression for the susceptibility. In Ref. 81, in the calculation of the corrections to χ and the heat capacity C_p the diagrams diverging as $q_m \to \infty$ were included in the coefficients of the model. With the help of such renormalized coefficients in the diagrams one can pass to the limit $q_m \to \infty$ and as a result the parameters appearing in the expressions for χ and C_p become the coefficients of the Landau–de Gennes model and T^*, but not q_m, as in Refs. 82 and 83.

The value $T_c - T^* \approx 1$ K was obtained from the analysis of the experimental data on the temperature dependence of the scattered light in 8CB liquid crystals ($C_8H_{1/2} - \quad - \quad - CN$) with $I^{-1}(\tau)$ approximated by a straight line. The use of q_m as an adjustable parameter[83] showed that the agreement between theory and experiment is very sensitive to the choice of the value of q_m. If q_m is taken to be the usual Debye value $q_m \sim 2\pi/l_0$, where l_0 is a dimension of the order of the intermolecular separation ($q_m \sim 5 \cdot 10^7$ cm^{-1}), $T_c - T$ was found to equal 0.03 °C, which is inconsistent with the experimental data, for example, on the correlation radius. To obtain $T_c - T^* \sim 1$ K values $q_m \sim 2.5 \cdot 10^6$ cm^{-1}, corresponding to a minimum size of the order of 100 Å, are necessary. In the opinion of Gramsbergen *et al.*[83] this size is somewhat too large.

In Ref. 81 the following expression, accurate up to terms of order τ^{-2}, was derived for $\chi(\tau)$:

$$\chi^{-1}(\tau) = a\tau \Big[1 + y_D - y_C \tau^{-1/2} - \Big(\frac{1}{7} y_C^2 - y_{BE} \Big) \times \tau^{-1} \ln \tau^{-1} - y_B \tau^{-3/2} + \frac{5}{14} y_B y_C \tau^{-2} - \frac{1}{2} y_B \Big(\frac{1}{7} y_C^2 - y_{BE} \Big) \times \tau^{-5/2} \ln \tau^{-1} - \frac{25}{63} y_B^2 \tau^{-3} \Big], \quad (6.8)$$

where

$$y_D = y_{D_1} + 18 y_{D_2}, \quad y_C = 7M \frac{C}{a}, \quad y_{BE} = \frac{77}{30} M^2 \frac{BE}{a^2},$$

$$y_B = \frac{7}{12} M \frac{B^2}{a^3}, \quad y_{D_i} = \frac{7}{2} M^2 \frac{D_i}{a} \quad (i = 1, 2), \quad M = \frac{k_B T}{4\pi a r_0^3}. \quad (6.9)$$

The region of applicability of these formulas, as an asymptotic expansion, is determined by the decrease of the corresponding terms. In particular, this condition obviously holds for

$$y_C \tau^{-1/2} \ll 1, \quad y_B \tau^{-3/2} \ll 1, \quad y_{BE} \tau^{-1} \ln \tau^{-1} \ll 1, \quad y_D \ll 1.$$

These inequalities play the role of the Ginzburg criterion for the given model. It is obvious from the expression for the susceptibility that the existence of fluctuation corrections owing to the cubic invariant $(1/3)\, B\, \mathrm{Sp}\, \hat{s}^3$ largely determines the behavior of the liquid crystal close to T_c.

The temperature dependence of R_{sc} can be described with the help of the formula (6.8) with an accuracy of the order of 1% in the entire measured range of temperatures. An analogous expression for the heat capacity also describes well the experiment[84] in the isotropic phase with the exception of the region of temperatures $T - T_c \leqslant 1$ K. These experiments and data on the temperature dependence of the average value of the order parameter $\varepsilon_a = \varepsilon_\parallel - \varepsilon_\perp$ in the nematic phase[85] were employed to determine the parameters of the Landau-de Gennes model. In particular, it was found that $a = 39 \pm 2$ J/cm^3 and $r_0 = 5.5$–6.5 Å. It is important to note that the coefficient C in the fourth-order term is negative. This indicates that terms right up to sixth order must be taken into account in (6.1) in order to ensure the stability of the system. In addition, it turned out that the model (6.1) with the parameters found describes well the behavior of ε_a as a function of temperature (with an accuracy of not less than 0.2%).

The analysis performed in Ref. 81 shows that the limiting critical behavior corresponding to the fluctuation region is not reached here, though the fluctuation corrections at $T \sim T_c$ are quite large. Thus for nematics existing in a wide region the employed approach enables describing experiments at all temperatures.

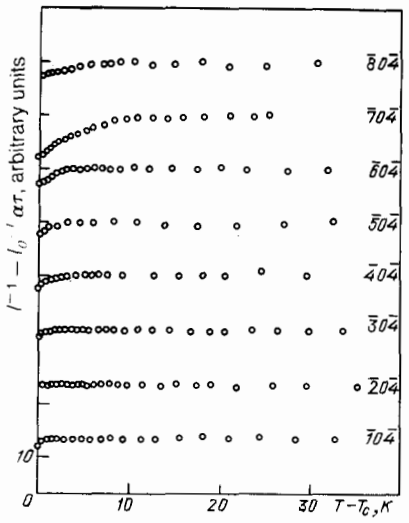

FIG. 14. Deviation of the temperature dependence of the inverse light scattering intensity in the isotropic phase of the NLC from the linear dependence $I^{-1} - I_0^{-1} A\tau$ in the homological series $\bar{n}04$.[86]

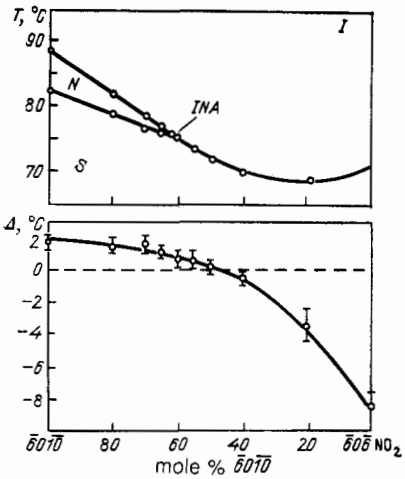

FIG. 15. Phase diagram and concentration dependence of the parameter Δ in the mixture of liquid crystals $\bar{6}01\bar{1}0$ and $60\bar{6}$ NO_2.[89,90] INA—triple point; *S*—smectic phase.

A more complicated picture is observed in the study of liquid crystals in which the nematic phase exists in a narrow temperature range. In this case the smectic A phase existing at lower temperatures may affect the intensity of light scattering. This question was discussed in a series of theoretical[86–88] and experimental[83,86,89] papers.

The temperature dependence of the intensity of the scattered light was measured in the homologous series of liquid crystals $\bar{n}0\bar{4}$ (4-*n*-oxybenzylidene-4′-*n*′-butylanalines), in which the width of the nematic phase varies from tens of degrees for $\bar{n} \sim 3$–4 up to several degrees for $\bar{n} \sim 6$–7 right up to complete vanishing of the nematic phase. The measurements are shown in Fig. 14, which shows the deviation of $I^{-1}(\tau)$ from a linear dependence. One can see from the figure that there is a correlation between the magnitude of the deviation and the width of the nematic phase.

In the study of scattering in a series of liquid crystals nCB (alkylcyanbiphenyls),[83] where the width of the nematic phase varies from 11 K for $n = 5$ to 1.7 K for $n = 7$, no such strong correlation, as in the case of the series of $\bar{n}0\bar{4}$, was observed, in spite of the strong deviation of the inverse susceptibility from linearity.

A somewhat different approach to this problem was employed in Refs. 89 and 90, where the scattering of light was studied in a mixture of the liquid crystals *p*-*n*-hexyloxyphenyl-*p*′-*n*-hexyloxynitrobenzoate ($\bar{6}0\bar{6}$ NO_2) and *p*-*n*-hexyloxyphenyl-*p*′-*n*-decanobenzoate (6010) in a wide range of concentrations. In this solution the width of the nematic phase can be smoothly varied from ~7 K with 100% of the nematic 6010 to zero for a concentration of the NLC 6010 of about 60 mole %. At lower concentrations of this nematic only the smectic A phase exists. The corresponding phase diagram is shown in Fig. 15.

The experimental data on the intensity of light scattering were analyzed on the basis of the model studied in Refs. 86–88. According to this model the Hamiltonian of the system in the isotropic phase of the liquid crystal near the transition point contains terms describing the nematic and smectic fluctuations as well as cross terms, responsible for their interaction. An expression was obtained for the inverse intensity of the scattered light in the single-loop approximation:

$$I^{-1} = I_0^{-1}\left[\frac{T - T_{IN}^*}{T_{IN}^*} - \frac{B_{NS}^2 T_{IN}^{*3/2}}{(T - T_{IN}^* + \Delta)^{3/2}}\right]\frac{T}{a},$$

where T_{IN}^* and T_{IS}^* are the temperatures of the divergence of the nematic and smectic fluctuations, respectively, in the absence of any interaction between them, $\Delta = T_{IN}^* - T_{IS}^*$, and B_{NS} is the interaction constant.

In analyzing the experiment the values of the parameters a, B_{NS}, Δ, and T_{IN}^*, which enable describing the experimental data in the entire temperature interval, were obtained.

The parameter Δ, which determines the slope of the susceptibility as a function of the temperature, is of greatest interest. Its values are presented in Fig. 14. One can see that near the triple point Δ is close to zero, and becomes negative as the nematic phase vanishes. This result corresponds to the fact that $T_{IS}^* > T_{IN}^*$, i.e., translational order strives to become established before the orientational order.

In the last few years studies of one other interesting class of liquid crystals—lyotropic nematic liquid crystals—have begun. These crystals arise owing to the interaction of nonspherical micelles (micellar solutions are discussed in detail in Sec. 7). The phase transition isotropic-liquid—nematic in lyotropic liquid crystals was studied in Refs. 91 and 92. In Ref. 91 the intensity of the scattered light and the birefringence Δn in a magnetic field H (Cotton-Mouton effect) in the liquid crystal decylammonia chloride (DAC), on the side of the isotropic phase, was measured. The inverse light scattering intensity and the ratio $H^2/\Delta n$ vary linearly with the temperature, and in addition $T_c - T^* = 0.8$ K. No deviation from linearity was observed. The coefficient a and r_0 were determined. It is interesting that $a \sim 1$ J/cm^3, i.e., it is 30 to 40 times smaller than in the usual NLC, while r_0 is somewhat larger, $r_0 = 16$ Å.

A recently synthesized lyotropic nematic is the compound cesium perfluoro-octanoate,[92] in a water solution of which the difference $T_c - T^* \sim 0.035 \pm 0.007$ K is very small. This value of $T_c - T^*$ was found from measurements of the Cotton-Mouton effect.[91] It is interesting to note that starting with $T - T_c \sim 2$ K the ratio $\Delta n/H^2$ depends on the intensity of the magnetic field, i.e., the next term H^4 must be taken into account in the dependence $\Delta n(H)$. The measured critical index γ turned out to equal 0.01 ± 0.04.

6.2. Kinetics of fluctuations of the order parameter in the isotropic phase of NLC

The kinetics of the tensor order parameter in the critical region has up to now been studied in less detail than the scalar order parameter. This is attributable to the fact that it is much more difficult to perform spectral measurements here, since the characteristic frequencies of the fluctuations of the order parameter are too high (of the order of several megahertz) for correlation spectroscopy, while on the other hand they are at the limit of resolution of modern Fabry-Perot etalons.

As in systems with a scalar order parameter, critical suppression of fluctuations is observed near the I-N transition point.[93] It was studied experimentally with the help of a Fabry-Perot confocal interferometer with the distance d between the mirrors of the order of several tens of centimeters. The use of the standard single-pass interferometer

with $d < 10$ cm does not make it possible to approach closer than 20–30 K to the transition point in liquid crystals such as MBBA.[94,95] The use of standard multipass interferometers appreciably extends the temperature range accessible to measurements. This is attributable to the fact that in such etalons the contrast, characterizing the ratio between the maximum and minimum intensity in the interference pattern, grows appreciably and reaches values, for example, of $\sim 10^7$ for the triple-pass etalons. The instrumental function of the multipass etalons drops off much more rapidly as a function of the frequency than the instrumental function of the standard interferometer, whose form is close to that of a Lorentzian contour.[13]

The idea of the method, enabling expansion of the frequency range accessible to measurements with multiple-pass etalons with a short base line d, is based on the difference in the shape of the physical signal (usually a Lorentzian contour or a contour close to it) and the instrumental function. The analysis is performed by the method of least squares using the entire block of data for the instrumental function and the spectral line under study.[96–98]

The typical temperature dependence of the relaxation time for MBBA is shown in Fig. 16. Unfortunately, the accuracy of the results obtained is not high enough to discuss the fine details of the nature of the kinetics of the I-N phase transition, as it is possible to do in the analysis of the integrated intensity.

The kinetics of the tensor order parameters described by the phenomenological equations proposed by de Gennes[73]:

$$\begin{aligned} -a\tau\delta\varepsilon_{\alpha\beta} &= 2\mu_0\dot{u}_{\alpha\beta} + \nu_0\dot{e}_{\alpha\beta}, \\ \sigma_{\alpha\beta} &= 2\eta_{s0}\dot{u}_{\alpha\beta} + 2\mu_0 e_{\alpha\beta}, \end{aligned} \tag{6.10}$$

where $\dot{u}_{\alpha\beta}$ is the strain rate tensor, $\sigma_{\alpha\beta}$ is the stress tensor, η_{s0} is the coefficient of shear viscosity at zero frequency, and μ_0 and ν_0 are phenomenological coefficients with the dimension of viscosity. The equations (6.10) represent the extension of the theory of Leontovich[99] to the case of liquid crystals.

These equations permit calculating the spectrum of the scattered light. In so doing the depolarized component $I_H^V(\omega)$, entirely determined by scattering by the fluctuations $\delta\varepsilon_{\alpha\beta}$, has the form

$$I_H^V(\omega) \sim \frac{[\omega^2 + \eta_{s\infty}\eta_{s0}(q^4/\rho^2)]\cos^2(\theta/2)}{[\omega^2 - (\eta_{s\infty}q^2/\rho\tau_\phi)]^2 + \omega^2[\tau_\phi^{-1} + (\eta_{s\infty}q^2/\rho)]} + \frac{\sin^2(\theta/2)}{\omega^2 + \tau_\phi^{-2}}, \tag{6.11}$$

where $\tau_f = \nu_0/a\tau$ is the oriented-relaxation time and $\eta_{s\infty} = \eta_{s0} - (2\mu_0^2/\nu_0)$ is the nonrelaxing part of the shear viscosity.

Study of the spectrum makes it possible, in principle, to determine all parameters appearing in the system of equations (6.10), if additional data on the static shear viscosity are employed, while the coefficient a is determined from the measurements of the integrated light scattering intensity as described above. In practice, however, this program is difficult to implement, since near T_c the form of the contour $I_H^V(\omega)$ does not differ much from a Lorentzian contour, and two parameters τ_b and η_{s0}, and then μ_0 and ν_0, must be found from it. There are two approaches to the solution of this problem. The parameters can be found by studying the spectrum $I_H^V(\omega)$ in the temperature range where the fine structure is observed,[95] after which the values found for μ_0 and ν_0 can be extrapolated into the critical region. Unfortunately the fine structure appears in MBBA at temperatures of the order of 150°C, which is approximately 100 K higher than T_c.

The other approach consists of performing additional experiments in the critical region. Such an experiment is the study of birefringence in a flow. As follows from Eq. (6.10), with our choice of $\delta\varepsilon_{\alpha\beta}$ for the order parameter, the optical anisotropy δn is related with the velocity gradient $\partial v_x/\partial z$ by the expression

$$\delta n = -\frac{\mu_0}{a\tau\bar{n}}\frac{\partial v_x}{\partial z}, \tag{6.12}$$

from which the coefficient μ_0 can be determined. In Ref. 100 the temperature dependence for τ_f and Maxwell's constant $M_0 = -\mu_0/a\tau\bar{n}$, were obtained for MBBA and BMOAB; they are described well by the relation $\exp(T_i/T)/(T - T^*)$, where $\exp(T_i/T)$ describes the noncritical temperature dependence, and in addition T_i are different for τ_f and M_0. The temperature dependence of μ_0 and ν_0 is shown in Fig. 17. The figure also shows the relaxing part of the shear viscosity:

$$\Delta\eta_s(\omega) = \frac{2\mu_0^2}{\nu_0}\frac{1}{1 + \omega^2\tau_f^2} \tag{6.13}$$

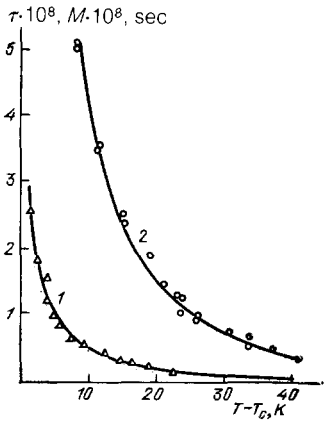

FIG. 16. Temperature dependence of Maxwell's constant (1) and the orientational relaxation time (2) in the isotropic phase of MBBA.[100]

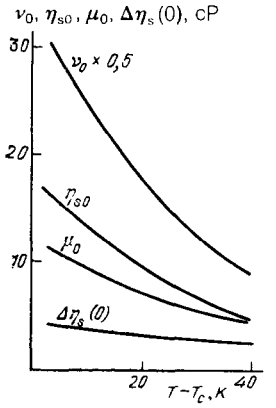

FIG. 17. Temperature dependence of the shear viscosity η_{s0}, the relaxing part $\Delta\eta_s(0)$ and the parameters of de Gennes' model μ_0 and ν_0 in MBBA.[100]

at zero frequency. One can see that $\Delta\eta_s$ is a weak function of the temperature, while the characteristic frequency $\omega_f = 1/\tau_f$ decreases in a critical manner. The orientational contribution to the viscosity $\Delta\tau_s$ is not large and, for example, in MBBA equals about 25%.

6.3. Light scattering in the nematic phase

The chief characteristic of the nematic phase is the existence of a predominant orientation of the molecules, characterized by the director vector **n**. Unlike systems with a scalar order parameter, in which fluctuations are associated with a local change in the number density of particles or the composition, fluctuations in the nematic phase arise owing to the local change in the orientational ordering. In this case the rotation of large groups of molecules, requiring small amounts of energy, occurs and for this reason such fluctuations are very large. As a result, strong light scattering is observed in the entire region of existence of the nematic phase, and R_{sc} is of the order of several inverse centimeters, which is 10^5–10^6 times greater than the standard noncritical light scattering.[73,101] Strictly speaking, the ordering in NLC is described by the angular distribution function of the molecular axes. In light scattering problems, however, to describe the order it is sufficient to use a symmetric traceless tensor of rank two $S_{\alpha\beta}$. The equilibrium value of this tensor $S^0_{\alpha\beta}$ in a uniaxial NLC has the form

$$S^0_{\alpha\beta} = S\left(n_\alpha n_\beta - \frac{1}{3}\delta_{\alpha\beta}\right). \tag{6.14}$$

As in the isotropic phase, $S_{\alpha\beta}$ is the dielectric permittivity tensor and S is the anisotropy of this tensor.

The fluctuations $\delta\varepsilon_{\alpha\beta}$

$$\delta\varepsilon_{\alpha\beta}(\mathbf{r}) = \varepsilon_{\alpha\beta}(\mathbf{r}) - \varepsilon^0_{\alpha\beta}$$

can be divided into three types[74]:

$$\delta\varepsilon_{\alpha\beta}(\mathbf{r}) = \delta\varepsilon^{\perp 1}_{\alpha\beta}(\mathbf{r}) + \delta\varepsilon^{\perp 2}_{\alpha\beta}(\mathbf{r}) + \delta\varepsilon^{\parallel}_{\alpha\beta}(\mathbf{r}), \tag{6.15}$$

where

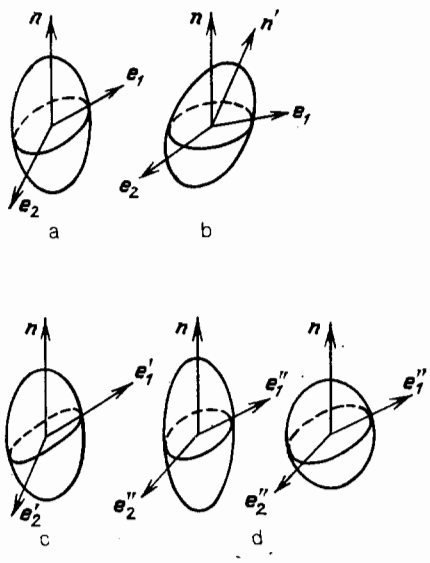

FIG. 18. Change in the dielectric ellipsoid for different types of fluctuations.

$$\delta\varepsilon^{\perp(1)}_{\alpha\beta}(\mathbf{r}) = \xi_1(\mathbf{r})(n_\alpha e_{1\beta} + n_\beta e_{1\alpha}) + \xi_2(\mathbf{r})(n_\alpha e_{2\beta} + n_\beta e_{2\alpha}),$$

$$\delta\varepsilon^{\perp 2}_{\alpha\beta}(\mathbf{r}) = \xi_3(\mathbf{r})(e_{1\alpha}e_{2\beta} + e_{1\beta}e_{2\alpha}) + \xi_4(\mathbf{r})(e_{1\alpha}e_{1\beta} - e_{2\alpha}e_{2\beta}),$$

$$\delta\varepsilon^{\parallel}_{\alpha\beta}(\mathbf{r}) = \xi_5(\mathbf{r})\left(n_\alpha n_\beta - \frac{1}{3}\delta_{\alpha\beta}\right); \tag{6.16}$$

here ξ_1, ξ_2, ξ_3, ξ_4, and ξ_5 are scalar variables and $\mathbf{e}_1$, $\mathbf{e}_2$, and $\mathbf{n}$ is a triplet of unit vectors of an orthogonal coordinate system. These fluctuations can be interpreted geometrically as changes occurring in a dielectric ellipsoid shown in Fig. 18.In Fig. 18(a) the ellipsoid is in an equilibrium state; in Fig. 18(b) $\delta\varepsilon^{\perp(1)}_{\alpha\beta}$ the ellipsoid rotates as a whole and these fluctuations are termed transverse uniaxial or fluctuations of the director; in Fig. 18(c) $\delta\varepsilon^{\perp 2}_{\alpha\beta}$ the ellipsoid of revolution transforms into a biaxial ellipsoid, corresponding to biaxial transverse fluctuations; in Fig. 18(d) $\delta\varepsilon^{\parallel}_{\alpha\beta}$ the ratio of the axes of the ellipsoid of revolution changes, i.e., these are longitudinal fluctuations corresponding to a change in the degree of anisotropy.[74,76]

It must be emphasized that from the viewpoint of molecular optics the nematic phase is a unique state of matter. On the one hand, in this system the optical anisotropy is significant, as in solids, while on the other hand the fluctuations of three types with completely different amplitudes and temperature dependence, which are expressed in terms of the fluctuations of the variables $\xi_1, \ldots, \xi_5$, are strongly developed. Fluctuations of ξ_1 and ξ_2 make the main contribution to scattering. In the Gaussian approximation

$$\langle|\xi_{i,\mathbf{q}}|^2\rangle = \frac{k_B T \varepsilon_a^2}{[K_{ii} + (K_{33} - K_{ii})\cos^2\theta]\, q^2}, \tag{6.17}$$

where K_{ii} $(i = 1, 2)$ and K_{33} are Frank's moduli, which are weakly temperature dependent. Fluctuations of this type are termed Goldstone fluctuations. They grow without bound as $q \to 0$, and in its entire region of existence the nematic phase is similar to the critical point itself with regard to fluctuations of the director.

Measurements in NLC are quite often performed in the presence of a magnetic field. In this case the fluctuations of ξ_1 and ξ_2 become finite as $\mathbf{q} \to 0$, since a term χH^2, where χ is the magnetic susceptibility, is added to the denominator in (6.17). The biaxial fluctuations of ξ_3 and ξ_4 do not have any singularities, while the fluctuations of ξ_5 grow in a critical manner as the N-I transition point is approach. As in the isotropic phase, their growth is disrupted by a first-order phase transition.[102]

The scattering of light by fluctuations of the director is the main type of scattering and is two to three orders of magnitude stronger than scattering by fluctuations of ξ_3, ξ_4, and ξ_5.[73,74] For this reason, we shall first study this—chief—scattering mechanism. The light-scattering function here is more complicated than for the standard isotropic media.[103,104] The intensity distribution in it depends not only on the scattering angle and the polarization, but also on the orientation of the director vector relative to the incident and scattered light. A detailed numerical analysis of these scattering functions in the presence of a magnetic field is performed in Ref. 104, where it is demonstrated that all three

Frank moduli can in principle be measured from the light-scattering data. As at the usual critical points the main distorting factor here is multiple scattering of light. In particular, the contribution of double scattering can reach 10% of the measured light-scattering intensity.[104]

There exist geometries of the experiment in which the contribution of single scattering by fluctuations of the director is zero.[4,73,74,76,105] Taking into account the optical anisotropy of the medium this is realized in the following cases:

$$\begin{aligned} &1)\ \boldsymbol{\alpha}\mathbf{n} = \boldsymbol{\beta}\mathbf{n} = 0, \\ &2)\ \boldsymbol{\alpha} \parallel \boldsymbol{\beta} \parallel \mathbf{n},\ \mathbf{k}_i\mathbf{n} = \mathbf{k}_s\mathbf{n} = 0, \\ &3)\ \mathbf{n} \parallel \mathbf{k}_n \pm \mathbf{k}_p; \end{aligned} \tag{6.18}$$

$\boldsymbol{\alpha}$ and $\boldsymbol{\beta}$ lie in the scattering plane. The vectors $\boldsymbol{\alpha}$ and $\boldsymbol{\beta}$ are the allowed directions of polarization of the incident and scattered light. The conditions 1 and 2 in (6.18) are most easily realized experimentally, since they correspond to the scattered components I_H^H and I_V^V with $\mathbf{n}$ oriented along the z axis (see Fig. 1).

The extinction coefficient also behaves in an unusual manner in the nematic phase. If it is defined as the integral over all scattering angles, then the presence of the pole $1/q^2$ in (6.17), where $\mathbf{q} = \mathbf{k}_i - \mathbf{k}_s$, should lead to a logarithmic divergence in σ as $\mathbf{k}_i \to \mathbf{k}_s$.[101] Because of the uniaxiality two types of rays can propagate in the NLC—ordinary (o) and extraordinary (e). The contribution to σ of the light wave polarized oppositely to the incident polarization is finite because the wave numbers $k^{(o)} = 2\pi n^{(o)}/\lambda$ and $k^{(e)} = 2\pi n^{(e)}/\lambda$ are unequal. For this reason only the scattered light with the same polarization as the incident light can make a diverging contribution to the integral. There may not be any divergence, however, if for geometric reasons there is no scattering at zero angle with coincident polarizations, i.e., the condition (6.18) holds for this angle. From the first condition in (6.18) it follows that this always holds for the ordinary ray. From the second condition it follows that for the extraordinary ray there is no divergence only if the angle ψ between $\mathbf{k}_i^{(e)}$ and $\mathbf{n}$ equals 90°.

For three such geometries $\mathbf{k}_i \| \mathbf{n}$; $\mathbf{k}_i \perp \mathbf{n}$, $\boldsymbol{\alpha} \perp \mathbf{n}$ and $\mathbf{k}_i \perp \mathbf{n}$, $\boldsymbol{\alpha} \| \mathbf{n}$ the extinction coefficient was measured in oriented magnetic fields from 10^3 to $3 \cdot 10^3$ G in MBBA samples 1–2 mm thick.[103] All Frank moduli were determined from the values obtained for the extinction coefficient and they are in good agreement with the measurements performed by other methods.

The angular dependence of the extinction coefficient of the ordinary ray in the presence of a magnetic field was calculated in Ref. 104 and without a magnetic field in Refs. 105 and 106. For the extraordinary ray for all angles of incidence ψ except $\psi = 90°$, the divergence in the limit of small angles remains. In the presence of a magnetic field, as already mentioned above, this divergence is removed by the term $1/(\chi H^2)$, and without a magnetic field the angles are cutoff at small angles $\theta_{min} \sim \lambda/L$, where L is the characteristic size of the system,[101,105,106] and in this case $\sigma^{(e)} \propto \ln(L/\lambda)$. The angular dependence of $\sigma^{(e)}$ is shown in Fig. 19. An analogous behavior is also obtained in the presence of a magnetic field.[104] Calculations of $\sigma^{(e)}$ by summation of the principal infrared divergences of the diagrams[101] show that $\sigma^{(e)}$ depends on the path length l traversed by the light in the medium $\sigma^{(e)}(l) \sim \ln(l/\lambda)$.

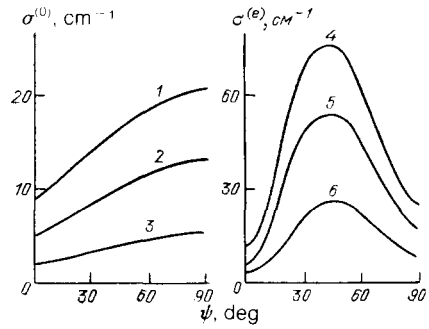

FIG. 19. The computed angular dependence of the coefficients of extinction of the ordinary $\sigma^{(o)}$ and extraordinary $\sigma^{(e)}$ rays.[105] 1, 4 BMOAB; 2, 5) MBBA; 3, 6) N-106.

The extinction coefficient for the extraordinary ray has not been measured experimentally. This is attributable to the fact that because of the extremely elongated scattering function almost all losses of light to scattering in the extraordinary ray occur owing to forward scattering by long-wavelength fluctuations of the director. As a result the extraordinary ray transforms, owing to multiple forward scattering, from a coherent into a diffusive ray with a small expansion of the light beam. Such a picture was observed by Val'kov *et al.*[106] experimentally and is shown in Fig. 20. This figure also shows a light ray with polarization (e), passing through the sample in the same plane as the oriented NLC N-106 about 2 mm thick for two angles of incidence ψ. The observed picture can be explained qualitatively by the sharp dependence of $\sigma^{(e)}$ on ψ (Fig. 19). The size of the central smeared spot reached 1°. The spot consisted of regions with different brightness, whose structure varied slowly with time. The characteristic times of these changes are deter-

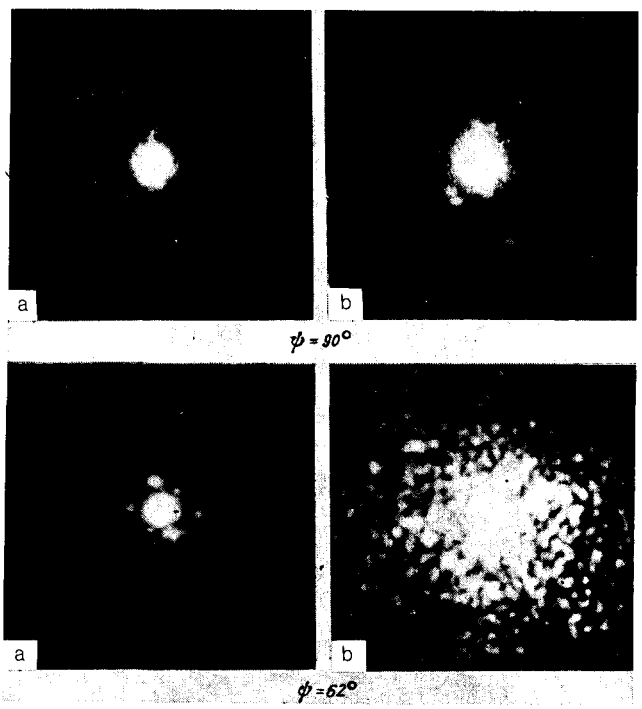

FIG. 20. Beam passing through a cell with planar orientation of N-106 liquid crystal 2 mm thick for two angles of incidence ψ.[106] a) ordinary beam, b) extraordinary beam.

mined by the kinetics of the long-wavelength fluctuations of the director[104] and reach fractions of a second at the center of the spot.

Thus the study of fluctuations of the tensor order parameter in NLC by optical methods has turned out to be very effective. The greatest progress was achieved in understanding the nature of the first-order phase transition I-N, though the experimental data are less informative than the usual critical phenomena owing to the fact that this transition is a first-order transition.

7. OPALESCENCE IN SEGREGATING MICELLAR SOLUTIONS AND MICROEMULSIONS

Most experimental facts regarding the usual critical points and phase transitions in liquid crystals have been explained theoretically in great detail. A somewhat different situation exists for segregating micellar solutions and microemulsions, which have been intensively studied experimentally in the last few years by the methods of molecular optics. Here there are many experimental facts that cannot yet be explained theoretically.

Micellar solutions are a heterogeneous system, one component of which are micelles—small colloidal particles containing from tens to thousands of elongated molecules. The main feature of these molecules is that the character of the interaction of their ends with the surrounding medium is significantly different. In particular, one end exhibits distinct polar properties. In cases of practical importance the surrounding medium is water, while the molecules are surfactants. In multicomponent systems the surfactants form a surface layer of micelles.

In the study of micellar solutions by optical methods far from the critical point the intensity of light scattering is written in the form[108]

$$I_V^V \sim \left(\frac{\partial n}{\partial \tilde{C}}\right)^2_{P,T} \tilde{C} k_B T \left(\frac{\partial \tilde{C}}{\partial \Pi}\right)_{P,T}, \qquad (7.1)$$

where $\tilde{C}$ is the volume fraction of micelles and Π is the osmotic pressure of the micellar component. The virial expansion is used for Π:

$$\Pi = \frac{\tilde{C} k_B T}{v_m} (1 + B\tilde{C} + \ldots), \qquad (7.2)$$

where v_m is the volume of a micelle and B is the second virial coefficient. The angular dependence is ignored, since the size of the micelles is much smaller than the wavelength of the light. If I_V^V is measured in absolute units as a function of the concentration, then the size of a micelle v_m as well as the second virial coefficient B, characterizing the interaction between micelles, can be determined. For the four-component system water–dodecane–sodium dodecylsulfate DCN–alcohol[2)] it turned out that the character of the interaction between the micelles depends on the length of the alcohol molecules: as the homological number of alcohol increases from C_5 to C_7 the attraction is replaced by repulsion. For a fixed number of alcohol molecules the force of attraction increases with the radius of the micelles r_m, the value of which was compared with the measurements of the extinction coefficient of the time correlation function $\Gamma = k_B T q^2 / 6\pi r_m \eta_s$.

Before we proceed to the analysis of critical phenomena in micellar solutions and microemulsions, we shall briefly study the main types of phase diagrams encountered. Figure 21 shows a typical phase diagram of a binary segregating micellar solution, where one of the components is a nonionogenic surfactant with the monomer

$$CH_3 (CH_2)_{i-1} - (OCH_2 - CH_2)_j OH$$

polyethylene glycol ester, which we shall denote as C_iE_j (in this case $i = 12, j = 8$), while the second component is water. In this diagram the region L_1 is the micellar solution, $L_1' + L_1''$ is the region of coexistence of two micellar solutions with different concentrations, and P_c is the lower critical point. The sharp asymmetry of the curve of coexistence of the phases L_1 and $L_1' + L_1''$ and the low value of C_c are often encountered in polymer solutions. This type of coexistence curve was obtained by a numerical method for spherical micelles by specially adjusting the interaction potential.[110] The region H corresponds to a lyotropic liquid crystal. The form of the diagram does not change much when the pressure is changed.

For the ternary system the phase diagram is shown schematically in Fig. 22,[111] which shows only the chief phase states of interest to us. To determine the composition of any point in the diagram a perpendicular must be dropped to the three sides of the triangle; the points of intersection determine the ratios between the three components of the mixture. As in Fig. 21, the phases L_1, $L_1' + L_1''$, and H are the microemulsion, a binary mixture of two microemulsions, and a liquid-crystalline phase; L_2 is an inverted microemulsion[112]; and P_c is the lower critical point of segregation. The areas referring to each phase vary with the temperature.

More complicated microemulsions are also now under intensive study. An example is the phase diagram for the mixture water–dodecane–pentanol in DCN.[113] In Fig. 23(a) the regions L_1, $L_1' + L_1''$, and H are the same as in Figs. 21 and 22; in addition, in this case H is a purely smectic phase, 98 wt. % of which is pentanol and dodecane. The x axis determines the ratio of the content of H_2O and DCN. A characteristic feature of this diagram is that at a fixed temperature there exists a line, bounded at two ends, of critical points $P_c^B P_c^A$. In addition, near the point P_c^A there exists a region where the smectic phase is in equilibrium with the micellar phases. The diagram in Fig. 23(b) illustrates the behavior of the solution as the temperature is varied with x held fixed. The figure clearly shows that the line $P_c^B P_c^A$ is the line of lower hypercritical points.

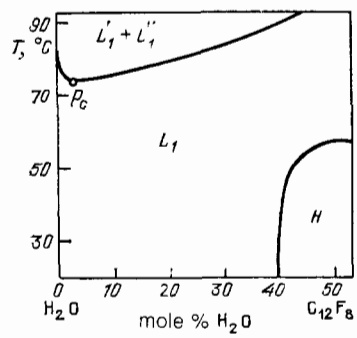

FIG. 21. Phase diagram of the system $C_{12}E_8$-H_2O.[109] L_1) micellar solution; $L_1' + L_1''$) segregated micellar solution; H) anisotropic phase; P_c is the lower critical point.

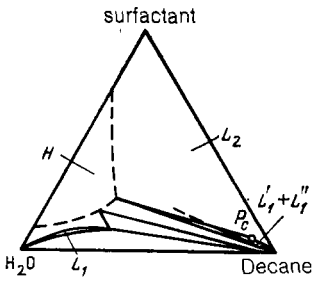

FIG. 22. Phase diagram of a ternary mixture at $T = 25°C$.[111] L_1) micellar solution; L_2) inverted micellar solution; H) anisotropic phase; $L_1' + L_1''$) segregated micellar solution; P_c is the lower critical point.

Extensive information on binary segregating micellar solutions as well as complex solutions consisting of four components, for which a quite large segment of the line of hypercritical points $P_c^A P_c^B$ was studied, has now been published. As regards ternary systems, the studied range of variation of their parameters is significantly narrower.

The dependence of the integrated intensity on the closeness to the critical point and the scattering angle as well as the time correlation function was studied by the method of light scattering. The critical indices in the binary solutions C_iH_j in H_2O and D_2O with the numbers of the homological series varying from $i = 6$ to 14 and $j = 3$ to 7 were obtained in Ref. 114. The extinction coefficient was measured in order to evaluate the magnitude of the multiple scattering. It was concluded that in the experimental geometry employed multiple scattering can be neglected only for $T - T_c > 0.2$ K. The values of the indices obtained for different terms of the homological series C_iE_j are given in Table IV. The table shows that the critical indices ν and γ decrease systematically as the sizes of the molecules C_iE_j increase while r_0 increases at the same time, and in addition the indices vary from scaling values to classical values and, what is most surprising, become less than the classical values. The simplest reason for this behavior could be the narrow temperature interval in which the measurements were performed. For this reason Corti *et al.*[114] performed additional studies in the system $C_{12}E_8 - H_2O$.[115] By reducing the size of the cell and thereby the intensity of multiple scattering of light they were able to obtain reliable results right up to $T - T_c \sim 0.02$ K. It turned out that the values of the critical indices ν and ρ_0 remained practically unchanged: $\gamma = 0.88 \pm 0.03$, $\nu = 0.43 \pm 0.03$, $r_0 = 23 \pm 3$ Å.

The system $C_{12}E_6 - H_2O$ was also studied by a different group.[116] For the temperature interval $5 \cdot 10^{-4} < \tau < 2 \cdot 10^{-2}$ the values of the indices obtained from the angular measurements turned out to equal $\gamma = 1.04 \pm 0.03$, $\nu = 0.51 \pm 0.01$ ($r_0 = 33 \pm 2$ Å), which agrees completely with the data presented in Table IV. In an adjacent interval $9 \cdot 10^{-5} < \tau < 5 \cdot 10^{-4}$ it was found that the temperature dependence of the susceptibility and correlation radius becomes weaker and is not described by simple power laws.

The experimental facts presented can now be interpreted as follows. For small numbers of the homologs (C_6E_3 and C_8E_4) in the vicinity of the critical point of segregation the intensity of light scattering increases owing to intensification of the concentration fluctuations, as in standard binary systems. Only one of the components here are micelles, whose shape and size do not change.

The appreciable decrease in γ and ν for longer molecules could be linked with the fact that, together with the usual critical phenomena, growth of micelles and a change in their shape from spherical to cylindrical occur. This picture is supported by the closeness of the critical point of mixing to the liquid-crystalline phase for large numbers of the homologs.

It is interesting to note that in micellar solutions the critical indices turned out to be sensitive to the isotopic composition of the solution.[115] Thus in the system $C_{12}E_8 - D_2O$ $\gamma = 1.20 \pm 0.03$, $\nu = 0.59 \pm 0.03$, $r_0 = 23 \pm 3$ Å, which differs appreciably from the values obtained in an analogous water solution (see Table IV). When a 50% mixture of H_2O and D_2O is used as the solvent intermediate values are obtained for the critical indices and ρ_0; this is attributed to the change in the degree of interaction of micelles with the solvent.

In addition, the shear viscosity η_s also behaves in an unusual fashion.[116] Measurements on a rotational viscosimeter for the mixture $C_{12}E_5 - H_2O$ showed that the shear viscosity depends strongly on the velocity gradient: $\eta_s \sim (\partial v_z/\partial x)^{-\omega}$, where $\omega = 0.13$ for $\tau \geqslant 5 \cdot 10^{-4}$ and $\omega \to 0.23$ for temperatures closer to T_c. Such values of ω are very different from the value obtained theoretically $\omega = 0.013$.[117] As a control Hamano *et al.*[116] measured η_s on the same apparatus for a standard segregating mixture and found that the effect is observed only very close to T_c, and in addition $\omega = 0.02$.

The index of the temperature divergence of the viscosity $x_\eta = 0.17$ is also anomalously large compared with the usual value for segregating mixtures $x_\eta \approx 0.06$.

Appreciable anomalies were also discovered in multicomponent systems. A four-component system was studied in greatest detail in Ref. 113. The existence of a line of phase-transition points $P_c^A P_c^B$ in Fig. 22(a) enables the study of the critical behavior of microemulsions with smoothly varying composition and therefore with different solution structure. The critical point was approached by two methods—by changing the mutual concentration of H_2O and DCN (the path I in Fig. 23(a)) and by changing the temperature with the composition held fixed (path II in Fig. 23(b)). The results of the measurements are given in Table V.

The values of the critical indices ν and γ decrease as the

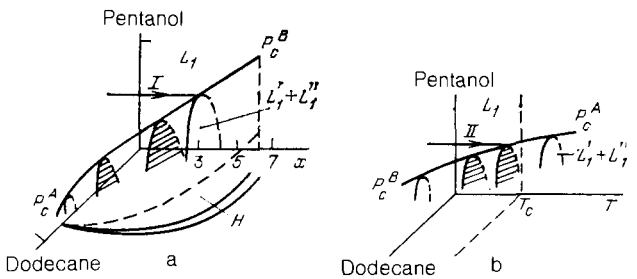

FIG. 23. Phase diagram of a quaternary binary mixture.[113] a) diagram for $T = \text{const}$; x is the ratio of DCN to H_2O; $P_c^B P_c^A$ is the line of the lower critical points; I) approach to the critical point by varying x. b) phase diagram with fixed x; II) approach to the critical point by varying the temperature; in both diagrams L_1 is the micellar solution, $L_1' + L_1''$ is the segregated micellar solution, and H is the smectic phase.

TABLE IV. Values of the critical parameters for different terms in the homological series.[114]

	C_6E_3	C_8E_4	$C_{12}E_6$	$C_{12}E_8$	$C_{14}E_7$
ν	0,63	0,57	0,53	0,44	
γ	1,25	1,15	0,97	0,92	0,87
r_0, Å	3.4	5.4	20	17,5	

concentration x decreases. Roux and Belloc[113] propose that this behavior of the critical parameters is linked, as for a binary system, with the existence of a smectic phase in the region of low concentrations; the closeness to this phase changes the values of ν and γ as a result of crossover.

For the ternary system the light-scattering intensity both as a function of the temperature and composition[111] was studied in a system whose phase diagram is shown in Fig. 21. The values of the indices ν and γ, found as the critical point is approached by varying the ratio $x = H_2O/$ surfactant, turned out to equal $\gamma_x = 1.26 \pm 0.06$, $\nu_x = 0.61 \pm 0.06$. Temperature measurements gave the values $\gamma_T = 1.30 \pm 0.05$, $\nu_T = 0.76 \pm 0.05$. In addition the value of ν turned out to be close to $\nu = 0.72 \pm 0.04$, found from scattering of slow neutrons.[118,119] Honorat *et al.*[111] explain the high values of ν and γ on the basis of the idea of the isomorphic nature of critical phenomena,[64,120,121] which leads to renormalization of the critical indices $\gamma_T \to \gamma/(1-\alpha)$, $\nu_T \to \nu(1-\alpha)$, where α is the critical index of the heat capacity.

The usual value $\nu = 0.62 \pm 0.03$ was obtained in temperature measurements by Abillon *et al.*[122] for a ternary mixture with a composition close to the above.

The kinetics of the critical fluctuations was studied by the methods of correlation spectroscopy. The approximation of the Kawasaki function (5.6) was employed for the decay constant. This approximation gives good agreement between theory and experiment.[109,111,114,122]

Although the results for micellar solutions and microemulsions deviate somewhat from the general picture, the basis for the interpretation of the experimental data from the viewpoint of critical phenomena is the existence of power laws for the susceptibility and correlation radius in a wide temperature interval. This is also supported by data on the kinetics of fluctuations, which is of a diffusion character, as in standard solutions.

8. CHARACTERISTICS OF LIGHT SCATTERING IN SYSTEMS WITH A CLOSED REGION OF SEGREGATION

Mixtures for which the coexistence curve is a closed region in the C, T plane and therefore contains two critical points—an upper critical point (UCP) and a lower critical point (LCP)—can be put into a separate class of segregating solutions. In some mixtures the size of the two-phase region can change appreciably as the pressure is varied or as low concentrations C_x of a third component are added. In the last few years a great deal of attention has been devoted[123-125] to the study of phase transitions in the system quaiacol (1-oxy-2-methoxybenzene $C_6H_4(OH)OCH_3$)—glycerine with a small addition of water. The phase diagram of this system in the coordinates C, T, and C_x is a dome-shaped surface, as shown in Fig. 24. As one can see from the figure, for each concentration C_x there exists a closed region of segregation, whose size depends on C_x. As C_x is decreased (z axis) the lines of the upper and lower critical points converge at the double critical point T_0. It should be noted that near this point at critical concentrations of quaiacol and glycerine the curve is symmetric in the C_x, T plane.

Theoretical analysis of this phase transition predicts that as the double critical point is approached all temperature indices are doubled owing to the change in the form of

TABLE V. Critical parameters in a four-component microemulsion.[113]

a) Approach to the critical point by varying the temperature

x_c	1.034	1.207	1,372	1,552	3,448	5,172
T_c, °C	36.35	37.54	34,52	32.25	33.43	35.47
ν_T	0.21±0,02	0.34±0.03	0.47±0,03	0,53±0.03	0.59±0,03	0.64±0,03
γ_T	0,40±0.04	0.63±0.06	0,87±0.06	1.01±0.06	1.14±0.06	1.24±0,06
r_0, Å	331±20	141±10	65±6	47±5	28±3	31±3

b) Approach to the critical point by varying the concentration

x_c	1.207	1.550	3.424
T_c, °C	21.84	25.4	21,80
ν_x	0.38±0.03	0.57±0.03	0.64±0,03
γ_x	0.78±0.06	1.10±0.06	1.20±0,06

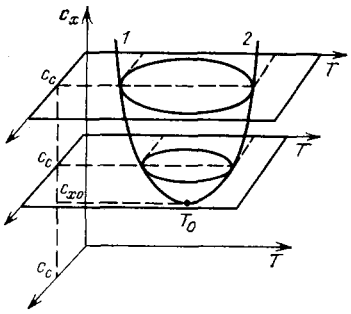

FIG. 24. Phase diagram of the system guaiacol-glycerine.[123] C is the concentration of the mixture, C_x is the concentration of water; 1, 2) line of the lower and upper critical points; T_0 is the binary critical point.

the first terms in the expansion of the free energy in powers of the order parameter.

The dependence of the properties of this solution on the width of the two-phase region ΔT has been studied experimentally. Jonston *et al.*[124] measured the intensity of the scattered light and its angular dependence as a function of the temperature in the single-phase region as the lower critical point is approached. The results of the measurements for the susceptibility are presented in Fig. 25. One can see that as the two-phase region decreases from 65.9° to 1.6° the index γ changes from the usual value 1.24 to practically twice this value. In the same work analogous results were obtained for the critical index ν from measurements of the scattering function.

The method of correlation spectroscopy was employed in Refs. 123 and 126 to determine the correlation radius on both sides of the region of segregation approaching both the lower and upper critical points. The critical indices ν were determined from the data shown in Fig. 26. It is interesting to note that within the limits of error for the given ΔT the values of ν_{UPC} and ν_{LCP} are the same and their maximum value equals $\nu = 1$ at $\Delta T = 1.3°$. Analogous growth of the index ν was discovered from experimental data on the temperature dependence of the shear viscosity.[127]

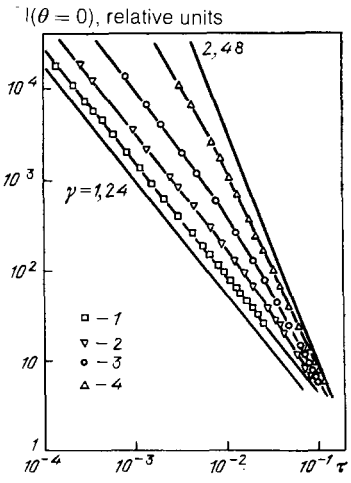

FIG. 25. Temperature dependence of the logarithm of the integrated intensity of scattered light at zero angle as a function of the logarithm of the reduced temperature with different width of the two-phase region ΔT.[124] 1) 65.9°C; 2) 26.3°C; 3) 9.4°C; 4) 1.6°C.

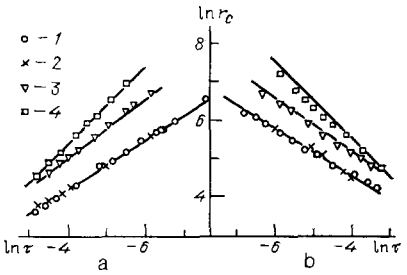

FIG. 26. The correlation radius as a function of the temperature as the lower (a) and upper (b) critical points are approached for different values of ΔT.[126] 1) 39.7°C; 2) 32.67°C; 3) 7.84°C; 4) 1.32°C.

In the study of a solution with $C_x < C_{x_0}$ (see Fig. 24), where a two-phase region does not exist, as expected, far from T_0 the susceptibility and correlation radius vary with the doubled values of the indices, while immediately beneath the dome their magnitude remains practically unchanged.

CONCLUSIONS

The foregoing review shows that the methods of light scattering are being increasingly employed to study phase transitions in the most diverse systems. This is attributable primarily to the fact that the recently developed technique of optical measurements of the scattered radiation intensity and its temporal characteristics has achieved an accuracy comparable with other thermodynamic and kinetic methods, and in some cases it has exceeded them. The results of optical experiments have contributed significantly to the formulation of modern ideas about the physical nature of phase transitions and critical phenomena. At the same time they have shown that there exists a number of problems concerning the fine details of the behavior of matter in the critical region, which are still being elucidated.

This refers primarily to the determination of the exact value of the index of anomalous dimensionality of the correlation function and clarification of the form of the correlation function, for which only exact asymptotic expressions in the region of small and large values of kr_C have been found. To determine the form of the correlation function in the entire range of values of kr_C experimentally, however, the accuracy with which the intensity is measured must be increased to 0.1%, just as for finding η.

In liquid crystals only the isotropic phase in the vicinity of the point of the transition into the nematic phase has been studied in greatest detail. Analogous measurements on the nematic phase side have practically not been performed; this is largely attributable to the smallness of the fluctuations, varying in a critical manner, compared with the usual fluctuations of the director. The more complicated and interesting cholesteric liquid crystals, where the phase transition into the ordered state is accompanied by strong optical effects (so-called blue phase), has still virtually not been studied by light-scattering methods.

Very little is as yet known about phase transitions in micellar solutions and microemulsions, and here further studies, both theoretical and experimental, must be performed and entirely different approaches to the description of the behavior of these unusual systems may have to be developed.

From the viewpoint of the experimental technique the study of critical opalescence has contributed greatly to the development of reliable and accurate methods for taking multiple scattering into account. This is attributable to the fact that in the critical region it is very easy to vary the level and characteristic size of nonuniformities. The application of these methods to strongly scattering systems of the most diverse nature appears to be very promising. This refers primarily to the optics of the atmosphere and ocean and the study of colloidal and biological systems, since here the same difficulties in acquiring information about the properties of the scattering nonuniformities appear as in the study of critical opalescence.

[1)]In what follows, in the case of scattering by fluctuations of the order parameter the index (C) for I, R_∞, and G will be dropped.

[2)]Micellar phases in ternary and quaternary systems are usually called microemulsions.

[1]a) M. A. Anisimov, *Critical Phenomena in Liquids and Liquid Crystals* [in Russian]. Nauka M. (1987); b) S. M. Rytov, Yu. A. Kravtsov, and V. I. Tatarskiĭ, *Introduction to Statistical Radio Physics* [in Russian]. Nauka M. (1978), Part II.

[2]E. L. Lakoza and A. V. Chalyĭ, Usp. Fiz. Nauk **140**, 393 (1988) [Sov. Phys. Usp. **26**, 573 (1983)].

[3]J. V. Sengers and J. M. B. Levelt Sengers, Ann. Rev. Phys. Chem. **37**, 189 (1986).

[4]A. Z. Patashinskiĭ and V. L. Pokrovskiĭ, Pergamon Press, Oxford (1979) [Russ. original, *Fluctuation Theory of Phase Transitions*, Nauka. M., 1975, 1982].

[5]D. W. Oxtoby and W. M. Gelbart, J. Chem. Phys. **60**, 3359 (1974).

[6]V. G. Puglielli and N. C. Ford Jr., Phys. Rev. Lett. **25**, 143 (1970).

[7]R. F. Chang, H. Burstyn, and J. V. Sengers, Phys. Rev. A **19**, 866 (1979).

[8]Yu. F. Kiyachenko, Author's Abstract of Candidate's Dissertation in Physical-Mathematical Sciences, All-Union Scientific-Research Institute of Physicotechnical and Radioelectronics Measurements, Moscow (1976).

[9]R. B. Kopelman and R. W. Gammon, Phys. Rev. A **29**, 2048 (1984).

[10]S. Chen. C. Lai, J. Rouch, and P. Tartaglia, *Ibid.* **27**, 1086 (1983).

[11]L. V. Adzhemyan, L. Ts. Adzhemyan, L. A. Zubkov, and V. P. Romanov, Zh. Eksp. Teor. Fiz. **78**, 1051 (1980) [Sov. Phys. JETP **51**, 530 (1980)].

[12]H. Z. Cummins and E. R. Pike [Eds.], *Photon Correlation and Light Beating Spectroscopy*, Plenum Press, N. Y., 1974 [Russ. transl., Mir. M., 1978].

[13]I. L. Fabelinskiĭ and I. L. Chistyĭ, Usp. Fiz. Nauk **119**, 487 (1976) [Sov. Phys. Usp. **19**, 597 (1976)].

[14]D. Beysens, A. Bourgou, and P. Calmettes, Phys. Rev. A **26**, 3589 (1982).

[15]L. V. Adzhemyan, L. Ts. Adzhemyan, L. A. Zubkov, and V. P. Romanov, Zh. Eksp. Teor. Fiz. **80**, 551 (1981) [Sov. Phys. JETP **53**, 278 (1981)].

[16]L. V. Adzhemyan, L. Ts. Adzhemyan, L. A. Zubkov, and V. P. Romanov, Zh. Eksp. Teor. Fiz. **83**, 539 (1982) [Sov. Phys. JETP **56**, 295 (1982)].

[17]M. A. Anisimov, A. V. Voronel', and T. M. Ovodova, Zh. Eksp. Teor. Fiz. **61**, 1092 (1971) [Sov. Phys. JETP **34**, 583 (1972)].

[18]M. E. Fisher, J. Math. Phys. **5**, 944 (1964).

[19]M. E. Fisher and J. S. Langer, Phys. Rev. Lett. **20**, 665 (1968).

[20]G. Stell, Phys. Lett. A **27**, 550 (1968).

[21]E. Bresin, D. J. Amit, and J. Zinn-Justin, Phys. Rev. Lett. A **32**, 151 (1974).

[22]M. E. Fisher and A. Aharony, Phys. Rev. B **10**, 2818 (1974).

[23]A. J. Bray and R. F. Chang, Phys. Rev. A **12**, 2594 (1975).

[24]R. A. Ferrell and D. J. Scalapino, Phys. Rev. Lett. **34**, 200 (1975).

[25]J. C. Le Guillou and J. Zinn-Justin, *Ibid.* **39**, 95 (1977).

[26]M. A. Anisimov, A. T. Berestov, V. P. Boronov, Yu. F. Kiyachenko, B. A. Koval'chuk, V. M. Malyshev, and V. A. Smirnov, Zh. Eksp. Teor. Fiz. **76**, 1660 (1979) [Sov. Phys. JETP **49**, 844 (1979)].

[27]M. J. Camp, D. M. Saul, J. P. Van Dyke, and M. Wortis, Phys. Rev. B **14**, 3990 (1976).

[28]F. J. Wegner, J. Phys. A **8**, 710 (1975).

[29]D. Beysens and G. Zalczer, Opt. Commun. **26**, 172 (1978).

[30]M. A. Anisimov, A. M. Evtyushenkov, Yu. F. Kiyachenko, and I. K. Yudin, Pis'ma Zh. Eksp. Teor. Fiz. **20**, 378 (1974) [JETP Lett. **20**, 170 (1974)].

[31]D. Schwahn, L. Belkovra, and D. Woermann, Ber. Bunsenges. Phys. Chem. **90**, 339 (1986).

[32]L. V. Adzhemyan, L. Ts. Adzhemyan, L. A. Zubkov, and V. P. Romanov, Pis'ma Zh. Eksp. Teor. Fiz. **22**, 11 (1975) [JETP Lett. **22**, 5 (1975)].

[33]L. A. Reith and H. L. Swinney, Phys. Rev. A **12**, 1094 (1975).

[34]Y. Garrabos, R. Tufeu, and B. Le Neidre, J. Chem. Phys. **68**, 495 (1978).

[35]L. Ts. Adzhemyan, I. A. Zubkov, and V. P. Romanov, Opt. Spektrosk. **52**, 91 (1982) [Opt. Spectrosc. (USSR) **52**, 54 (1982)].

[36]L. V. Adzhemyan, L. Ts. Adzhemyan, L. A. Zubkov, and V. P. Romanov, Opt. Spektrosk. **46**, 967 (1979) [Opt. Spectrosc. (USSR) **52**, 545 (1979)].

[37]J. P. Shoetler, D. M. Kim, and R. Kobayashi, Phys. Rev. A **27**, 1134 (1983).

[38]H. C. Burstyn, J. V. Sengers, J. K. Bhattacharjee, and R. A. Ferrell, Phys. Rev. A **28**, 1567 (1983).

[39]P. C. Hohenberg and B. I. Halperin, Rev. Mod. Phys. **49**, 435 (1977).

[40]K. Kawasaki, Ann. Phys. (N. Y.) **61**, 1 (1970).

[41]K. Kawasaki, Phase Transitions and Critical Phenomena, Academic Press, New York (1975), Vol. 5A, p. 165.

[42]L. V. Adzhemyan, L. Ts. Adzhemyan, and V. P. Romanov, Teor. Mat. Fiz. **27**, 104 (1976) [Theor. Math. Phys. **27**, 362 (1976)].

[43]T. Ohta, Prog. Theor. Phys. **54**, 1556 (1975).

[44]T. Ohta and K. Kawasaki, *Ibid.* **55**, 1384 (1976).

[45]E. G. Siggia, B. I. Halperin, and P. C. Hohenberg, Phys. Rev. B **13**, 2110 (1976).

[46]K. Kawasaki and S. M. Lio, Phys. Rev. Lett. **29**, 48 (1975).

[47]G. Paladin and L. Peliti, J. Phys. (Paris) Lett. **43**, L-15 (1982).

[48]H. C. Burstyn and J. V. Sengers, Phys. Rev. A **25**, 448 (1982).

[49]C. M. Sorensen, R. C. Mockler, and W. J. O'Sullivan, Phys. Rev. Lett. **40**, 777 (1978); Opt. Commun. **20**, 140 (1977); Phys. Rev. A **16**, 365 (1977).

[50]R. F. Chang, P. H. Keyes, J. V. Sengers, and C. O. Alley, Phys. Lett. **27**, 1706 (1971).

[51]K. Hamano, T. Nomura, T. Kawazura, and N. Kuwahara, Phys. Rev. A **26**, 1153 (1982).

[52]A. Stein, J. C. Allegra, and G. F. Allen, J. Chem. Phys. **55**, 4265 (1971).

[53]C. M. Sorensen, Int. J. Thermophys. **3**, 365 (1982).

[54]B. C. Tsai and D. McIntyre, J. Chem. Phys. **60**, 937 (1974).

[55]K. Hamano, S. Teshigawara, T. Koyana, and N. Kuwahara, Phys. Rev. A **33**, 485 (1986).

[56]H. C. Burstyn, J. V. Sengers, and P. Esfadiari, *Ibid.* **22**, 282 (1980).

[57]H. Guttinger, and D. S. Cannell, *Ibid.*, 285.

[58]J. K. Bhattacharjee and R. A. Ferrell, *Ibid.* **23**, 1511 (1981).

[59]H. C. Burstyn, R. F. Chang, and J. V. Sengers, Phys. Rev. Lett. **44**, 410 (1980).

[60]H. C. Burstyn and J. V. Sengers, Phys. Rev. A **27**, 1071 (1983).

[61]V. P. Romanov and T. Kh. Salikhov, Opt. Spektrosk. **58**, 1091 (1985) [Opt. Spectrosc. (USSR) **58**, 666 (1985)].

[62]R. A. Ferrell and J. K. Bhattacharjee, Phys. Rev. A **19**, 348 (1979).

[63]D. Beysens and G. Zalczer, *Ibid.* **15**, 765 (1977).

[64]M. A. Anisimov, Usp. Fiz. Nauk **114**, 249 (1974) [Sov. Phys. Usp. **17**, 722 (1974)].

[65]K. Kawasaki and Y. Shiva, Physica A **113**, 27 (1982).

[66]L. V. Adzhemyan, L. Ts. Adzhemyan, V. P. Romanov, and V. A. Solov'ev, Akust. Zh. **25**, 23 (1979) [Sov. Phys. Acoust. **25**, 12 (1979)].

[67]Y. Garrabos, G. Zalczer, and D. Beysens, Phys. Rev. A **25**, 1147 (1982).

[68]G. N. Kolesnikov, V. S. Starunov, and I. L. Fabelinskiĭ, *Acoustical Spectroscopy, Quantum Acoustics, and Acoustoelectronics* [in Russian], Physics Institute of the Academy of Sciences, Tashkent, 1978, p. 226.

[69]M. A. Anisimov, V. P. Voronov, and V. M. Malyshev, Pis'ma Zh. Eksp. Teor. Fiz **18**, 224 (1973) [JETP Lett. **18**, 133 (1973)].

[70]L. Ts. Adzhemyan, V. P. Romanov, and T. Kh. Salikhov, Opt. Spektrosk. **58**, 339 (1985) [Opt. Spectrosc. (USSR) **58**, 202 (1985)].

[71]S. Beysens and G. Zalczer, Opt. Commun. **26**, 172 (1978).

[72]L. Ts. Adzhemyan, L. A. Zubkov, and V. P. Romanov, Opt. Spektrosk. **52**, 91 (1982) [Opt. Spectrosc. (USSR) **52**, 54 (1982)].

[73]P. de Gennes, *The Physics of Liquid Crystals*, Clarendon Press, Oxford, 1974 [Russ. transl. Mir. M. (1977)].

[74]V. L. Pokrovskii and E. I. Kats, Zh. Eksp. Teor. Fiz. **73**, 774 (1977) [Sov. Phys. JETP **46**, 405 (1977)].

[75]S. A. Pikin, *Structural Transformations in Liquid Crystals* [in Russian], Nauka. M. (1982).

[76]A. Yu. Val'kov and V. P. Romanov, Zh. Eksp. Teor. Fiz. **83**, 1777 (1982) [Sov. Phys. JETP **56**, 1028 (1982)].

[77]R. L. Stratonovich, Zh. Eksp. Teor. Fiz. **70**, 1290 (1976) [Sov. Phys. JETP **43**, 672 (1976)].
[78]T. W. Stinson and J. D. Litster, Phys. Rev. Lett. **30**, 688 (1973).
[79]T. W. Stinson and J. D. Litster, *Ibid.* **25**, 503 (1970).
[80]E. Gulary and B. Chy, J. Chem. Phys. **62**, 795 (1975).
[81]L. V. Adzhemyan, L. Ts. Adzhemyan, A. Yu. Val'kov, L. A. Zubkov, I. V. Mel'nik, and V. P. Romanov, Zh. Eksp. Teor. Fiz. **87**, 1244 (1984) [Sov. Phys. JETP **60**, 712 (1984)].
[82]M. J. Stephen and C. P. Fan, Phys. Rev. Lett. **25**, 500 (1970).
[83]E. F. Gramsbergen, L. Longa, and W. H. de Jeu, Phys. Rept. **135**, 195 (1986).
[84]M. A. Anisimov, V. M. Mamnitskii, and E. L. Sorkish, Inzh. Fiz. Zh. **39**, 1100 (1980).
[85]I. Haller, H. A. Huggins, H. R. Liliental, and T. R. McGuire, J. Phys. Chem. 77, 950 (1973).
[86]A. Gohin, C. Destrude, H. Gusparoux, and J. Prost. J. Phys. (Paris) **44**, 427 (1983).
[87]M. A. Anisimov, E. E. Gorodetskiĭ, and V. E. Podnek, Pis'ma Zh. Eksp. Teor. Fiz. **37**, 352 (1983) [JETP Lett. **37**, 414 (1983)].
[88]E. E. Gorodetskiĭ and V. E. Podnek, Kristallografiya **29**, 1054 (1984) [Sov. Phys. Crystallogr. **29**, 618 (1984)].
[89]M. A. Anisimov, V. I. Labko, G. L. Nikolaenko, and I. K. Yudin, Mol. Cryst. Liq. Cryst. Lett. **2**, 77 (1985).
[90]M. A. Anisimov, V. N. Labko, G. A. Nikolaenko, and I. K. Yudin, Pis'ma Zh. Eksp. Teor. Fiz. **45**, 88 (1987) [JETP Lett. **45**, 111 (1987)].
[91]S. Kumar, J. D. Litster, and C. Rosenblatt, Phys. Rev. A **28**, 1890 (1983).
[92]C. Rosenblatt, *Ibid.* **32**, 1115 (1985).
[93]T. W. Stinson and J. P. Litster, J. Appl. Phys. **41**, 996 (1970).
[94]T. D. Gierke and V. H. Flugare, J. Chem. Phys. **61**, 2231 (1974).
[95]G. R. Alms, T. D. Gierke, and G. D. Patterson, *Ibid.* **67**, 5779 (1977).
[96]J. Vanderval, S. M. Mudare, and D. Walton, Opt. Commun. **37**, 33 (1981).
[97]L. V. Adzhemyan, L. Ts. Adzhemyan, L. A. Zubkov, N. V. Orekhov, and V. P. Romanov, Opt. Spektrosk. **59**, 1169 (1985) [Opt. Spectrosc. (USSR) **59**, 701 (1985)].
[98]C. H. Wang, R. I. Ma, and Q. L. Lin, J. Chem. Phys. **80**, 617 (1984).
[99]M. A. Leontovich, J. Phys. USSR **4**, 499 (1941).
[100]L. A. Zubkov, N. V. Orekhova, V. P. Romanov, and S. V. Alimov, Zh. Eksp. Teor. Fiz. **92**, 859 (1987) [Sov. Phys. JETP **65**, 484 (1987)].
[101]L. D. Landau and E. M. Lifshitz, *Electrodynamics of Continuous Media*, Pergamon Press, N. Y., 1984 [Russ. original, Nauka, M., 1982].
[102]M. J. Stephen and J. P. Straley, Rev. Mod. Phys. **46**, 615 (1974).
[103]D. Langevin and M. A. Bouchiat, J. Phys. (Paris) **36**, Colloq. Nr. C-1, 195 (1975).
[104]E. Miraldi, I. Trossi, and P. Taverna Valabreda, Nuovo Cimento B **60**, 165 (1980).
[105]A. Yu. Val'kov and V. P. Romanov, Zh. Eksp. Teor. Fiz. **90**, 1264 (1986) [Sov. Phys. JETP **63**, 737 (1986)].
[106]A. Yu. Val'kov, I. A. Zubkov, A. P. Kovshik, and V. P. Romanov, Pis'ma Zh. Eksp. Teor. Fiz. **40**, 281 (1984) [JETP Lett. **40**, 1064 (1984)].
[107]L. Ts. Adzhemyan, A. N. Vasil'ev, and Yu. M. Pis'mak, Teor. Mat. Fiz. **68**, 323 [Theor. Math. Phys. **68**, 855 (1986)].
[108]S. Brunetti, D. Roux, A. M. Bellocq. G. Fourche, and P. Bothorel, J. Phys. Chem. **87**, 1028 (1983).
[109]V. Gegiorgio, R. Piazza, M. Corti, and C. Minero, J. Chem. Phys. **82**, 1025 (1985).
[110]L. Reatto and M. Tau, Chem. Phys. Lett. **108**, 292 (1984).
[111]P. Honorat, D. Roux, and A. M. Bellocq, J. Phys. (Paris) Lett. **45**, 961 (1984).
[112]K. L. Mittal [Ed.], *Micellization, Solubilization, and Microemulsions*, Plenum Press, N. Y., 1977 [Russ. transl. Mir. M., 1980].
[113]D. Roux and A. M. Bellocq, Chem. Phys. Lett. **94**, 156 (1983).
[114]M. Corti, C. Minero, and V. Gegiorgio, J. Phys. Chem. **88**, 309 (1984).
[115]M. Corti and V. Gegiorgio, Phys. Rev. Lett. **55**, 2005 (1985).
[116]K. Hamano, T. Sato, T. Koyama, and N. Kuwahara, *Ibid.*, 1472.
[117]A. Onuki and K. Kawasaki, Phys. Lett. A **75**, 485 (1981).
[118]J. S. Huang and M. W. Kim, Phys. Rev. B **26**, 2703 (1982).
[119]M. Kotlarchyak, S. H. Chen, J. S. Hyang, and M. W. Kim, Phys. Rev. A **29**, 2054 (1984).
[120]B. Widom, J. Chem. Phys. **46**, 3324 (1967).
[121]R. B. Griffits and J. C. Wheeler, Phys. Rev. A **2**, 1047 (1970).
[122]D. Abillon, D. Chatenay, D. Langevin, and J. Meuneir, J. Phys. (Paris) Lett. **45**, L223 (1984).
[123]S. V. Krivokhizha, O. A. Lugovaya, I. L. Fabelinskiĭ, and L. L. Chaikov, Zh. Eksp. Teor. Fiz. **89**, 85 [Sov. Phys. JETP **62**, 48 (1985)].
[124]R. G. Jonston, N. A. Cloark, P. Wiltzius, and D. S. Cannell, Phys. Rev. Lett. **54**, 49 (1985).
[125]J. S. Walker and C. A. Vause, J. Chem. Phys. **79**, 2660 (1983).
[126]V. P. Zaĭtsev, S. V. Krivokhizha, I. L. Fabelinskiĭ, A. Tsitrovskiĭ, L. L. Chaikov, E. V. Shvets, and P. Yani, Pis'ma Zh. Eksp. Teor. Fiz. **43**, 85 (1986) [JETP Lett. **43**, 112 (1986)].
[127]S. V. Krivokhizha and L. L. Chaikov, Kr. Soobshch. Fiz., FIAN SSSR, No. 9, 50 (1985) [Sov. Phys. Lebedev Inst. Rep. No. 9, 53 (1985)].

Translated by M. E. Alferieff